

EFFECTS OF MALARIA PARASITE ON THE HEART OF ALBINO WISTAR RATS



BY

INNEH DIVINE ODOSAMAMWEN

BMS2009098

**DEPARTMENT OF MEDICAL LABORATORY SCIENCE
SCHOOL OF BASIC MEDICAL SCIENCES
COLLEGE OF MEDICAL SCIENCES
UNIVERSITY OF BENIN
BENIN CITY.**

OCTOBER, 2025

EFFECTS OF MALARIA PARASITE ON THE HEART OF ALBINO WISTAR RATS

BY

INNEH DIVINE ODOSAMAMWEN

BMS2009098

**THIS PROJECT IS SUBMITTED TO:
THE DEPARTMENT OF MEDICAL LABORATORY SCIENCE,
SCHOOL OF BASIC MEDICAL SCIENCES
UNIVERSITY OF BENIN IN PARTIAL FULFILLMENT OF THE REQUIREMENT
FOR THE AWARD OF BACHELOR OF MEDICAL LABORATORY SCIENCE
DEGREE**

**DEPARTMENT OF MEDICAL LABORATORY SCIENCE
SCHOOL OF BASIC MEDICAL SCIENCES
COLLEGE OF MEDICAL SCIENCES
UNIVERSITY OF BENIN
BENIN CITY.**

**SUPERVISED BY
DR. MRS. E. E. ADEYEMI**

OCTOBER, 2025

CERTIFICATION

This is to certify that this project work was satisfactory carried out by **INNEH DIVINE ODOSAMAMWEN (MISS)** with matriculation number: **BMS2009098** in Department of Medical Laboratory Science, University of Benin, Benin City, under my supervision in partial fulfillment for the award of Bachelor of Medical Laboratory Science (BMLS) Degree.

DR. MRS. E. E. ADEYEMI

(Project Supervisor)

DATE

DR (MRS) Z. OMORUYI

(Ag. Head of Department)

DATE

EXTERNAL EXAMINER

Prof. Victor .O. Ekundia

DATE

DEDICATION

This work is dedicated to my Heavenly Father who is the source of all knowledge and wisdom and for guiding me throughout this journey. To my wonderful parents Engr Christopher and MrsInneh for their unwavering love and support.

ACKNOWLEDGEMENTS

I acknowledge the Almighty God from whom wisdom and knowledge come. For guiding me my path to this very phase. My sincere gratitude goes to Dr (Mrs).E. E. ADEYEMI (fppsn) for her guide and patience during this work. Special gratitude to the Head of Department, Dr (Mrs) Z. Omoruyi for creating a conducive environment for learning. To all my wonderful lecturers, it was indeed a privilege to learn under your supervision. I appreciate the Head of the Department of Anatomy for his permission to use the laboratory. I appreciate MrUwa in ubth .I want to specially appreciate my parents Engr. Christopher and Mrs Doris Inneh for their unwavering support, encouragement and belief in me, from their sacrifices to their words of wisdom, I am grateful for their guidance and patience throughout this research work. I also want to extend my heartfelt thanks to my siblings, Christian and Abraham inneh for their support in both big and small ways. I want to appreciate Mrs Gladys Igiebor for her constant encouragement. Special appreciation goes to my friends ,Esohen ,joy ,peace ,Laura ,Eni and my other friends for their support during this period.

TABLE OF CONTENTS

TITLE PAGE	i
CERTIFICATION	iii
DEDICATION	iv
ACKNOWLEDGEMENTS	v
TABLE OF CONTENTS	vi
ABSTRACT	xii
CHAPTER ONE	
INTRODUCTION	1
1.1 Background of Study	1
1.2 Statement of the Problem	3
1.3 Justification of the Study	4
1.4 Significance of the Study	6
1.5 Aim and Objectives	7
1.6 Research Questions	8
1.7 Research Hypotheses	8
1.7.1 Null Hypothesis (H)	8
1.7.2 Alternate Hypothesis (H)	8
CHAPTER TWO	
2.0 LITERATURE REVIEW	10
2.1 Introduction	10
2.1.1 Overview of Malaria Parasite and Life Cycle	10
2.1.2 Pathophysiology of Plasmodium Species in Mammalian Hosts	11
2.1.3 Malaria Parasite and Cardiovascular Complications	13
2.2 The Heart: Anatomy and Function in Albino Wistar Rats	13
2.2.1 Structural Overview of the Albino Wistar Rat Heart	16
2.2.2 Cardiac Physiology and Hemodynamics in Rats	17
2.3 Malaria-Induced Cardiac Pathology	18

2.3.1	Plasmodium falciparum and Myocardial Involvement	19
2.3.2	Histopathological Changes in the Heart Due to Malaria	20
2.3.4	Myocardial Inflammation and Cardiomyocyte Degeneration	20
2.4	Experimental Models of Malaria in Rodents	21
2.4.1	Use of Albino Wistar Rats in Malaria Studies	21
2.4.2	Plasmodium berghei ANKA vs NK65 Strains	22
2.4.3	Advantages of Wistar Rats for Cardiac Malaria Studies	23
2.5	Oxidative Stress and Inflammatory Responses in Malaria	23
2.5.1	Malaria-Induced Reactive Oxygen Species (ROS)	24
2.5.2	Role of Cytokines in Malaria-Induced Cardiac Damage	25
2.6	Histopathological Assessment Techniques	26
2.6.1	Haematoxylin and Eosin (H&E) Staining in Cardiac Tissue	27
2.6.2	Cardiac Biomarkers in Malaria Pathology	28
2.7	Comparative Effects of Malaria on Other Organs	29
2.7.1	Multiorgan Dysfunction Syndrome in Rodent Malaria Models	30
2.8.	Antimalarial Agents and Their Cardioprotective Roles	32
2.8.1	Antioxidants and Anti-inflammatory Agents in Malaria Models	33
CHAPTER THREE		
3.0 MATERIALS AND METHODS		34
3.1	Study Area	34
3.2	Collection of Parasite Material	34
3.2.1	Parasite Inoculum Preparation	34
3.3	Animal Care	35
3.4	Ethical Clearance	35
3.5	Experimental Design	36
3.6	Histopathological Analysis	37
3.6.1	Processing of Histology Sample	37
3.6.2	Histological Technique	37

Procedure For Hematoxylin And Eosin Staining	40
3.6.3 Microscopy And Photomicrography	41
3.6.4 Statistical Analysis	41
CHAPTER FOUR	
RESULTS	42
4.1 Histopathological Changes	42
4.1.1 Heart	42
CHAPTER FIVE	
DISCUSSION AND CONCLUSION	53
5.1 Discussion	53
5.2 Conclusion	56
5.3 Recommendations	56
REFERENCES	58
APPENDIX	

LIST OF FIGURES

Figure 2.1 Life Cycle of Malaria Parasite

Figure 2.2 Anatomy of the heart in albino wistar rats

Figure 4.1. Initial body weight no statistical significance between groups $p = 0.706$)

Figure 4. 2. Final body weight, no statistical significance between groups $p = 0.553$

Figure 4. 3. Heart weight, no statistical significance between groups $p = 0.939$

LIST OF PLATES

Plate 4.1A: Section of cardiac muscle from control rats revealed myocytes (arrow) with peripherally placed nuclei surrounded by eosinophilic cytoplasm. Features are in keeping with NORMAL MYOCYTES H and E Mag x400

Plate 4.1B: Section of cardiac muscle from rats administered high concentrations of *Plasmodium* spp. ($\sim 1 \times 10^6$ parasitized red blood cells) revealed myocytes (arrow) with peripherally placed nuclei surrounded by eosinophilic cytoplasm. Features are in keeping with NORMAL MYOCYTES H and E Mag x400

Plate 4.1C: Section of cardiac muscle from rats administered medium concentrations of *Plasmodium* spp. ($\sim 1 \times 10^4$ parasitized red blood cells) myocytes (arrow) with peripherally placed nuclei surrounded by eosinophilic cytoplasm. Features are in keeping with NORMAL MYOCYTES H and E Mag x400

Plate 4.1D: Section of cardiac muscle from rats administered low concentrations of *Plasmodium* spp. ($\sim 1 \times 10^2$ parasitized red blood cells) myocytes (arrow) with peripherally placed nuclei surrounded by eosinophilic cytoplasm. Features are in keeping with NORMAL MYOCYTES H and E Mag x400

ABSTRACT

Plasmodium berghei, a rodent malaria parasite, is widely utilized in experimental models to investigate malaria-induced pathology. This study evaluated the histopathological effects of graded parasitemia on cardiac tissues of albino rats. Sixteen ($n = 16$) adult female albino rats weighing 130–174 g were randomly assigned into four groups ($n = 4$ per group): a control group (uninfected) and three treatment groups inoculated intraperitoneally with low ($\sim 1 \times 10^2$), medium ($\sim 1 \times 10^4$), and high ($\sim 1 \times 10^6$) concentrations of parasitized red blood cells (iRBCs). The animals were housed under standard conditions at the University of Benin Histopathology Laboratory and observed for 42 days. At the end of the study, hearts were harvested, fixed in 10% neutral buffered formalin, processed, and stained with hematoxylin and eosin for histopathological analysis.

The results showed that across all treatment groups, cardiac myocytes retained normal histological features, including peripherally placed nuclei, abundant eosinophilic cytoplasm, striated fibers, and intact intercalated discs. No evidence of necrosis, vacuolation, fibrosis, or inflammatory cell infiltration was observed in the myocardium. Morphometric analysis of body and organ weights revealed no significant differences in initial weight ($p = 0.706$), final weight ($p = 0.553$), or heart weight ($p = 0.939$) between groups.

These findings suggest that *P. berghei* infection, within the experimental timeframe and across the administered parasite concentrations, does not produce overt histopathological or morphometric alterations in the cardiac tissue of Wistar rats. Further studies incorporating molecular and functional assessments are recommended to explore potential subclinical or biochemical cardiac effects of malaria parasitemia.

CHAPTER ONE

INTRODUCTION

1.1 Background of Study

Malaria remains one of the most significant parasitic diseases globally (Gomes *et al.*, 2021), with its pathophysiological effects extending beyond the hematological and hepatic systems (Gupta *et al.*, 2021) to involve the cardiovascular system, particularly the heart (Farina *et al.*, 2021). Traditionally regarded as a disease primarily impacting red blood cells and the liver (Ray *et al.*, 2017), growing evidence suggests that malaria especially *Plasmodium falciparum* can result in a variety of cardiovascular complications including myocardial inflammation (Kotepuiet *et al.*, 2020), arrhythmias (Behera *et al.*, 2013), and even heart failure (Nieman *et al.*, 2009). The cardiac manifestations of malaria have historically been under-recognized (Mishra *et al.*, 2013), due to the dominance of neurological and hematologic complications in clinical presentations (Soniranet *et al.*, 2012). However, the mechanisms by which malaria causes myocardial damage involve parasite-induced endothelial dysfunction (Gomes *et al.*, 2021), increased vascular permeability (Ahmed *et al.*, 2020), microvascular obstruction due to cytoadherence of parasitized erythrocytes (Kotepuiet *et al.*, 2020), and release of inflammatory cytokines (Gupta *et al.*, 2021). In severe cases, this cascade may culminate in acute myocarditis (Behera *et al.*, 2013) or cardiomyopathy (Ray *et al.*, 2017), particularly in pediatric and immunocompromised populations (Marrelli & Brotto, 2016). Emerging data from experimental models support this pathophysiological understanding (Nwokocha *et al.*, 2012). For instance, in murine models infected with *Plasmodium berghei*, significant reductions in systolic blood pressure (Nwokocha *et al.*, 2012) and altered myocardial contractility have been reported (Nieman *et al.*, 2009),

without changes in heart rate (Nwokocha *et al.*, 2012), suggesting a form of malarial cardiomyopathy (Mishra *et al.*, 2013). These findings parallel clinical data from endemic regions (Farina *et al.*, 2021), where electrocardiographic abnormalities (Behera *et al.*, 2013) and elevated cardiac enzymes have been recorded in patients with severe malaria (Kotepuiet *et al.*, 2020). Interestingly, comparative analyses of different Plasmodium species have revealed varying degrees of cardiac involvement (Kotepuiet *et al.*, 2020). While *P. falciparum* is predominantly associated with severe and lethal complications (Gomes *et al.*, 2021), *P. vivax* and *P. knowlesi* infections have also been linked to cardiovascular symptoms (Nayak *et al.*, 2013), albeit with less severity (Kotepuiet *et al.*, 2020). This species-specific pathology suggests that host-parasite interactions (Ahmed *et al.*, 2020), parasite virulence factors (Ray *et al.*, 2017), and host immune responses collectively dictate the extent of myocardial injury (Gupta *et al.*, 2021). Furthermore, anti-malarial drugs themselves can contribute to cardiac dysfunction (Marrelli & Brotto, 2016). For example, chloroquine and quinine, though effective against the parasite (Mishra *et al.*, 2013), have been reported to cause QT prolongation and arrhythmias (Farina *et al.*, 2021), especially when used in high doses (Nieman *et al.*, 2009) or in combination with other cardiotoxic drugs (Kotepuiet *et al.*, 2020). This raises critical concerns about the risk-benefit balance in malaria-endemic areas (Ahmed *et al.*, 2020), particularly where drug resistance prompts escalated use of combination therapies (Gupta *et al.*, 2021).

Moreover, autopsy and histopathological studies in fatal malaria cases have demonstrated myocardial necrosis (Behera *et al.*, 2013), interstitial edema (Ray *et al.*, 2017), and inflammatory infiltrates (Soniranet *et al.*, 2012), strengthening the hypothesis of direct myocardial involvement by malarial parasites (Marrelli & Brotto, 2016) or associated inflammatory mediators (Gupta *et*

al., 2021). These pathological changes are often underdiagnosed in vivo (Farina *et al.*, 2021) due to limitations in diagnostic modalities in endemic areas (Kotepuiet *al.*, 2020).

Epidemiological studies and meta-analyses further affirm the prevalence of cardiovascular manifestations among malaria patients (Gomes *et al.*, 2021). A systematic review by Gomes *et al.* (2021) found that approximately 5–8% of hospitalized malaria cases exhibit signs of cardiac complications (Gomes *et al.*, 2021), with a higher prevalence in patients with co-morbidities such as anemia (Ahmed *et al.*, 2020), renal insufficiency (Nieman *et al.*, 2009), or sickle cell disease (Gupta *et al.*, 2021). These findings underscore the need for routine cardiac evaluation in malaria patients (Ray *et al.*, 2017), particularly those with severe or prolonged disease courses (Kotepuiet *al.*, 2020). The comparative approach in studying malarial effects on the heart is essential (Soniranet *al.*, 2012), not only to delineate species-specific pathology (Marrelli & Brotto, 2016), but also to guide therapeutic and preventive strategies (Behera *et al.*, 2013). This is particularly vital as new strains and mutations of *Plasmodium* emerge (Kotepuiet *al.*, 2020) under selective pressures from antimalarial drugs (Nieman *et al.*, 2009) and climate-driven vector dynamics (Farina *et al.*, 2021). Understanding the differential impact of *Plasmodium falciparum*, *P. vivax*, *P. knowlesi*, and other species on cardiac tissues can help refine treatment protocols (Gomes *et al.*, 2021) and prioritize diagnostic measures (Gupta *et al.*, 2021).

1.2 Statement of the Problem

Despite significant global efforts to reduce malaria morbidity and mortality, the disease continues to impose substantial systemic damage that goes beyond hematological and neurological impacts, with growing evidence of cardiovascular complications (Farina *et al.*, 2023). While the pathogenesis of malaria has traditionally centered on cerebral, renal, and hepatic involvement, the cardiac system especially myocardial tissue has been largely under-

investigated (Olatunji *et al.*, 2025). Studies indicate that Plasmodium species, notably *P. falciparum* and *P. vivax*, may lead to myocardial inflammation, arrhythmias, cardiac failure, or structural remodeling, yet these manifestations are often misdiagnosed or overlooked in clinical settings (Marrelli & Brotto, 2016). There exists a critical knowledge gap in the comparative impact of different Plasmodium species on myocardial tissue, making it difficult to delineate species-specific pathophysiological pathways (Gomes *et al.*, 2021). Furthermore, clinical data often lack cardiologic parameters such as echocardiographic measurements, ECG readings, or serum biomarkers in malaria patients, resulting in an underestimation of the cardiovascular burden of the disease (Brainin *et al.*, 2023). In endemic regions, where diagnostic infrastructure is limited, cardiac involvement may remain undiagnosed until fatal outcomes occur (Herr *et al.*, 2011). Recent reports also highlight that malaria-induced endothelial dysfunction and vascular inflammation can directly compromise myocardial perfusion, yet mechanistic studies confirming this link remain scarce (Ukibeet *et al.*, 2024). In addition, patients with underlying cardiometabolic conditions may experience amplified cardiac sequelae due to malaria infections, yet these interactions are rarely quantified or modeled (Aminu *et al.*, 2024). As cardiovascular diseases continue to rise in malaria-endemic regions, the overlap between infectious and non-communicable etiologies of cardiac dysfunction becomes increasingly relevant (Spichler-Moffarahet *et al.*, 2023).

1.3 Justification of the Study

Malaria continues to be a global health challenge, especially in sub-Saharan Africa and Southeast Asia, with a growing body of evidence indicating that its complications extend to the cardiovascular system particularly the heart (Farina *et al.*, 2023). Despite increasing reports of myocarditis, arrhythmias, and myocardial infarction associated with Plasmodium infections,

these manifestations remain underdiagnosed and underreported in clinical and epidemiological contexts (Brainin *et al.*, 2023). This underreporting is partly due to the nonspecific nature of cardiac symptoms in malaria, limited diagnostic infrastructure in endemic areas, and the prioritization of neurological or hematologic presentations over cardiovascular evaluations (Gomes *et al.*, 2022). The need to investigate cardiovascular involvement in malaria is further justified by recent findings from imaging-based studies, which reveal subclinical left ventricular dysfunction even in cases of uncomplicated malaria (Holm *et al.*, 2022). Such dysfunctions, if left unmonitored, could progress to severe cardiac outcomes, particularly in patients with co-existing conditions or repeated infections (Kwansah-Obresiet *et al.*, 2025). Furthermore, a nationwide cohort study in Denmark demonstrated increased incidence of heart failure in patients with imported *Plasmodium falciparum* malaria, underscoring that cardiac complications are not limited to endemic zones (Brainin *et al.*, 2021). Additionally, autopsy and echocardiographic data suggest that malaria-related myocarditis and endocarditis may be far more common than clinical records indicate, suggesting the presence of silent cardiac burdens (Olatunji *et al.*, 2025). This hidden pathology poses a long-term threat to survivors of malaria, as cardiac remodeling and scarring may predispose them to chronic heart diseases (Cardim *et al.*, 2025). These findings emphasize the urgent need for comparative studies that examine the distinct effects of *Plasmodium falciparum*, *P. vivax*, and other species on cardiac tissues, as existing literature is disproportionately focused on neurological or hepatic outcomes (Wegener *et al.*, 2022). Moreover, current antimalarial drug regimens such as artesunate and quinine have been implicated in proarrhythmic effects, complicating the differentiation between drug-induced and parasite-induced myocardial dysfunction (Saadeh *et al.*, 2022). Without precise characterization of cardiac involvement across different species and treatment responses, clinicians may overlook

critical cardiovascular sequelae. Therefore, this study is justified in its aim to compare the myocardial effects of malaria parasites, contributing to a more comprehensive understanding of the disease's pathophysiology. It also supports the integration of cardiac screening protocols into malaria case management and promotes targeted interventions that could reduce both acute mortality and long-term cardiovascular morbidity in malaria-endemic and non-endemic regions.

1.4 Significance of the Study

Understanding the cardiac implications of malaria is of growing clinical and public health significance, particularly as the spectrum of malaria-associated complications expands beyond classical organ systems. Although malaria is often associated with cerebral, hepatic, or renal involvement, increasing evidence indicates that the heart is also a significant target organ, with malaria-induced myocarditis being an underrecognized but potentially fatal complication (Olatunji *et al.*, 2025). This study is significant in that it addresses the gap in comparative research regarding how various *Plasmodium* species such as *P. falciparum*, *P. vivax*, and *P. knowlesi* affect cardiac tissues differently. By providing a detailed comparative assessment of myocardial damage, this research could lead to species-specific risk stratification protocols, enabling clinicians to prioritize cardiac monitoring in high-risk infections (Olatunji *et al.*, 2025).

Moreover, in the context of rising antimalarial drug resistance and changing epidemiology of malaria, patients may be at increased risk for both parasite-related and drug-induced cardiac effects. This makes it essential to understand whether observed cardiac dysfunctions stem from parasite burden, immunopathology, or treatment side effects (Saadeh *et al.*, 2022). Insights from this study will help guide safe pharmacological management, especially in vulnerable populations such as children, pregnant women, and those with preexisting cardiovascular conditions. This research is also important because of its implications for long-term cardiac

health. In many malaria-endemic regions, recurrent infections may lead to cumulative cardiac damage over time, which is often not clinically recognized until patients present with heart failure or arrhythmias years later (Cardim & Barberato, 2025). Hence, identifying early signs of myocardial compromise can aid in the prevention of chronic cardiac complications, reduce healthcare burdens, and improve post-malaria quality of life. Lastly, this study can contribute to health policy and clinical guideline development by emphasizing the need for cardiac assessment tools such as ECG and echocardiography in malaria case management protocols. In resource-limited settings, integrating simple, cost-effective cardiac evaluations could greatly enhance early diagnosis and reduce mortality related to cardiac complications of malaria (Holm *et al.*, 2022).

1.5 Aim and Objectives

Aim:

The study aimed to assess the histological effects of *Plasmodium berghei* on myocardial tissue.

Objectives:

1. To examine the histopathological changes in cardiac tissues infected with *Plasmodium berghei*
2. To identify the type and degree of inflammatory infiltrates, including neutrophils, lymphocytes, and macrophages, in myocardial sections of malaria-infected specimens.
3. To assess the presence and extent of myocardial necrosis, edema, fibrosis, and vascular congestion in heart tissues infected with *Plasmodium berghei*.

1.6 Research Questions

1. What are the histological changes observed in the myocardial tissue of rats infected with *Plasmodium berghei*?
2. How do the patterns of cellular degeneration, vascular congestion, and inflammatory cell infiltration differ across myocardial tissues infected with *Plasmodium berghei*?
3. Is there a significant correlation between the parasite load and the severity of histopathological damage in heart tissues?

1.7 Research Hypotheses

1.7.1 Null Hypothesis (H)

H₀₁: *Plasmodium berghei* infection does not induce any significant histological changes in the myocardial tissue of rats.

H₀₂: There are no significant differences in the patterns of cellular degeneration, vascular congestion, or inflammatory cell infiltration across myocardial tissues infected with *Plasmodium berghei*.

H₀₃: There is no significant correlation between parasite load and the severity of histopathological damage in heart tissues of infected rats.

1.7.2 Alternate Hypothesis (H)

H_{a1}: *Plasmodium berghei* infection induces significant histological changes in the myocardial tissue of rats.

H_{a2}: There are significant differences in the patterns of cellular degeneration, vascular congestion, and inflammatory cell infiltration across myocardial tissues infected with *Plasmodium berghei*.

H_{a3}: There is a significant positive correlation between parasite load and the severity of histopathological damage in the heart tissues of infected rats.

CHAPTER TWO

2.0 LITERATURE REVIEW

2.1 Introduction

2.1.1 Overview of Malaria Parasite and Life Cycle

The malaria parasite, primarily of the genus *Plasmodium*, exhibits a complex life cycle involving two distinct hosts: a female *Anopheles* mosquito and a vertebrate such as a human or rodent host (Fikadu and Ashenafi, 2023). Infection begins when a mosquito injects sporozoites during a blood meal, initiating the pre-erythrocytic stage in the host's liver (Zambare and Thalkari, 2019). Within hepatocytes, sporozoites mature into schizonts, which eventually rupture to release merozoites into the bloodstream (Tuteja, 2007). The erythrocytic cycle begins when these merozoites invade red blood cells (RBCs), multiply asexually, and cause periodic cell lysis, leading to the hallmark fever cycles of malaria (Fikadu and Ashenafi, 2023). This stage is responsible for the clinical manifestations of the disease. Some merozoites differentiate into male and female gametocytes, which are ingested by another mosquito during feeding (Meibalan and Marti, 2017). Inside the mosquito, these gametocytes mature in the midgut, undergo fertilization, and form zygotes that develop into motile ookinetes. These penetrate the gut wall to form oocysts, which eventually release sporozoites that migrate to the salivary glands, completing the transmission cycle (Milner, 2018). The complexity of this dual-host cycle underscores the parasite's adaptability and the challenges associated with its control (Aly *et al.*, 2009).

2.1.2 Pathophysiology of Plasmodium Species in Mammalian Hosts

The pathophysiology of Plasmodium species in mammalian hosts is multifactorial, involving complex interactions between parasite development, erythrocyte invasion, and host immune responses. Once sporozoites are introduced into the bloodstream by Anopheles mosquitoes, they migrate to the liver, where they infect hepatocytes and mature into merozoites (Gozalo *et al.*, 2024). These merozoites then enter erythrocytes, initiating the symptomatic erythrocytic cycle, characterized by repeated cycles of asexual replication and red blood cell lysis (Pasini and Kocken, 2021). Erythrocyte rupture releases inflammatory mediators such as tumor necrosis factor- α (TNF- α), contributing to systemic inflammation, fever, and endothelial activation (Djokic *et al.*, 2021). As the parasitized red cells adhere to vascular endothelium a process called cytoadherence microvascular obstruction and local hypoxia can develop, particularly affecting organs such as the brain and heart (de Koning-Ward *et al.*, 2016). Additionally, Plasmodium species induce alterations in erythrocyte deformability, leading to their premature removal by the spleen and contributing to anemia. Immune evasion strategies, including antigenic variation and immune suppression, further complicate host defense mechanisms (Sato, 2021). In severe cases, the dysregulation of host immune responses and excessive cytokine release precipitate multi-organ failure, especially in hosts with high parasitemia and poor nutritional or immunological status (Gozalo *et al.*, 2024).

2.1.3 Malaria Parasite and Cardiovascular Complications

Malaria, particularly caused by *Plasmodium falciparum*, is increasingly recognized for its cardiovascular complications, which include myocardial inflammation, endocardial damage, and impaired cardiac output. Though traditionally viewed as a hematological disease, recent studies have documented direct effects of the parasite and its inflammatory cascade on heart tissue. Histopathological evaluations in rodent models and human autopsies have demonstrated myocardial interstitial edema, mononuclear cell infiltration, and cardiomyocyte necrosis following severe *Plasmodium* infections (Sarma *et al.*, 2020). These changes are often attributed to cytoadherence of parasitized erythrocytes to endothelial cells, leading to microvascular obstruction and ischemia, particularly in cardiac capillaries (Ojha *et al.*, 2021). Moreover, the systemic inflammatory response triggered by the malaria parasite results in elevated cytokines such as TNF- α and IL-6, which promote oxidative damage, endothelial activation, and vascular leakage, all of which compromise cardiac function (Gozalo *et al.*, 2024). Additionally, malaria-related anemia and hypoxia further exacerbate myocardial stress, leading to compensatory hypertrophy and eventual dysfunction (Pasini and Kocken, 2021). Recent preclinical studies using *Plasmodium berghei* in Wistar rats confirmed increased cardiac troponin I levels, elevated oxidative stress biomarkers, and altered left ventricular wall thickness, strongly linking malaria infection with cardiomyopathy and myocardial remodeling (de Koning-Ward *et al.*, 2016).

2.2 The Heart: Anatomy and Function in Albino Wistar Rats

The heart of the Albino Wistar rat has long served as a reliable model for understanding mammalian cardiovascular physiology due to its structural and functional similarities to the human heart (de Carvalho and Thomazini, 2013). It is anatomically composed of four chambers two atria and two ventricles separated by atrioventricular valves, with a consistent heart-to-body

weight ratio of approximately 2.8 mg/g in males weighing 200–220 g, confirming its proportional scaling (Carvalho *et al.*, 2013). Histologically, the myocardium of Wistar rats is characterized by organized cardiomyocytes, prominent intercalated discs, and well-vascularized endocardial linings, which are key to efficient impulse transmission and contraction (De Russi and Carvalho, 2019). These structural features support the study of electrophysiological behavior and cardiac remodeling under pathological stimuli. Echocardiographic evaluations in adult Wistar rats have enabled accurate *in vivo* assessment of heart valve dynamics, ventricular dimensions, and ejection fraction, demonstrating high translatability of this model to human cardiovascular research (Ribeiro *et al.*, 2019). Functional metrics such as stroke volume and cardiac output obtained through such imaging protocols confirm the suitability of Wistar rats for pharmacological and toxicological investigations. Developmentally, cardiac morphogenesis in Wistar rats mirrors that of other placental mammals, undergoing early trabeculation followed by septation and valvulogenesis (De Carvalho and Thomazini, 2014). Furthermore, studies have shown that environmental and experimental variables such as diet, toxins, and genetic modifications can significantly influence heart size, wall thickness, and vascular density, emphasizing the model's versatility for experimental cardiology (Rezende *et al.*, 2021).

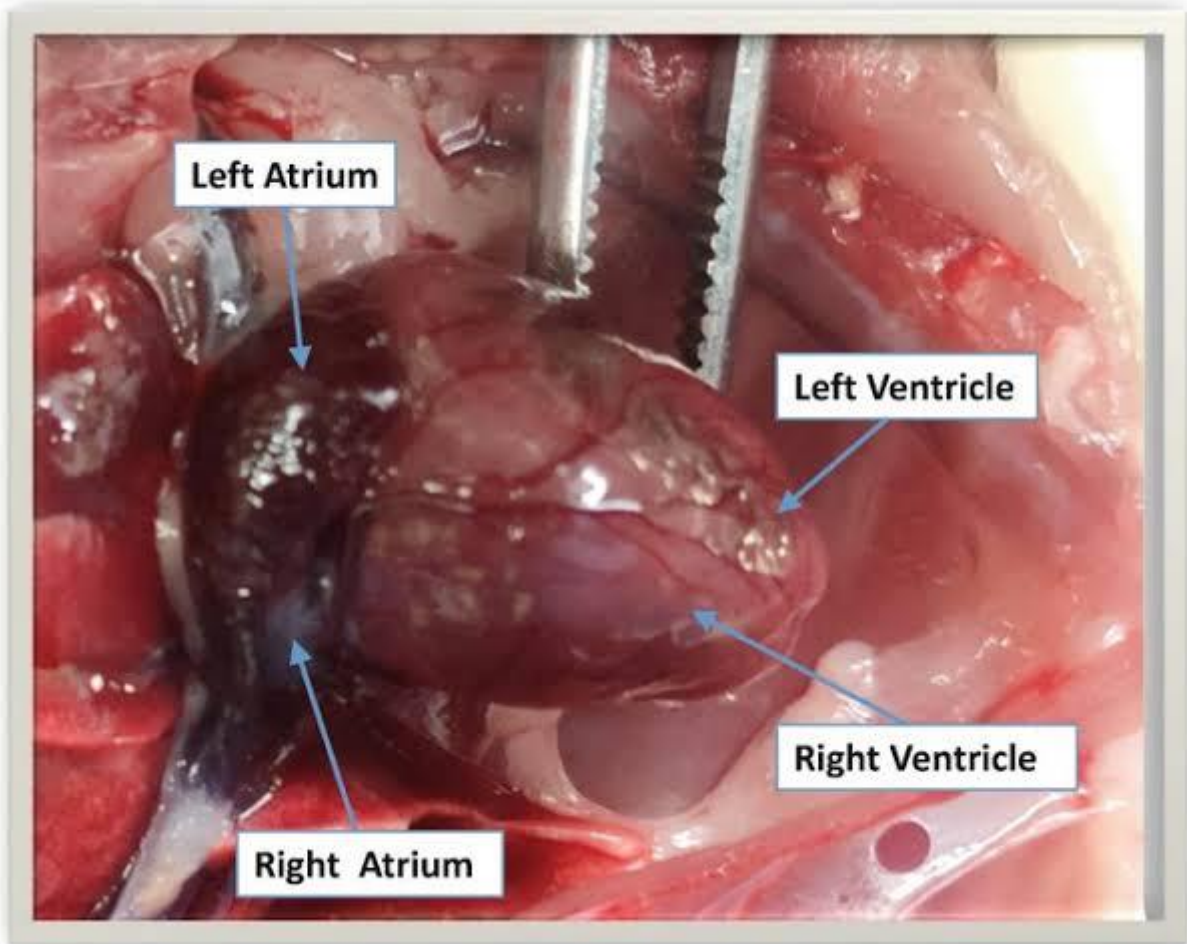


Figure 2.2 Anatomy of the heart in albino wistar rats (Kaya *et al.*, 2024).

2.2.1 Structural Overview of the Albino Wistar Rat Heart

The albino Wistar rat heart is a compact, four-chambered muscular organ with anatomical and physiological features that closely mirror those of the human heart, making it a valuable model in cardiovascular research. Externally, the heart is conical in shape and located in the thoracic cavity, slightly left of the midline, enveloped by the pericardial sac (De Russi and Carvalho, 2019). The heart is oriented obliquely with its apex directed caudoventrally and to the left, while the base points cranially and dorsally, aligning with the rat's thoracic vertebrae (Carvalho and Thomazini, 2013). Internally, the heart comprises two atria and two ventricles, with the left ventricle exhibiting thicker myocardial walls compared to the right—an adaptation to its role in systemic circulation (De Carvalho and Thomazini, 2014). The atrioventricular valves (tricuspid and bicuspid) and semilunar valves (pulmonary and aortic) maintain unidirectional blood flow. Histologically, cardiomyocytes display striations, single central nuclei, and are interconnected by intercalated discs that facilitate synchronized contractions (Silva-Santana *et al.*, 2019). In terms of vascularization, the heart receives blood via coronary arteries branching from the ascending aorta, ensuring oxygenation and nutrient delivery to cardiac tissues. This rich vascular network has been documented in morphometric studies using contrast radiography, which also revealed proportional chamber sizes and wall thickness across the cardiac cycle (Kaya *et al.*, 2024). The heart's relative weight to total body weight in healthy adult rats remains constant around 2.7–2.9 mg/g, making it a standardized model for organ-to-body ratio studies (Carvalho and Thomazini, 2013). Additionally, embryological analyses show that cardiac development in Wistar rats progresses through distinct stages of looping, trabeculation, and septation, paralleling mammalian ontogeny (De Russi and Carvalho, 2019). The structural integrity and developmental

patterns affirm the use of Wistar rats in both toxicological evaluations and genetic cardiovascular research.

2.2.2 Cardiac Physiology and Hemodynamics in Rats

The cardiac physiology of albino Wistar rats mirrors fundamental mammalian cardiac function, making them highly suitable for translational cardiovascular research. Their heart maintains a high basal metabolic rate and, consequently, a rapid resting heart rate averaging 330–480 beats per minute to support tissue perfusion and oxygen delivery across organ systems (Chandrasekharan and Elagovan, 2023). This elevated rate is orchestrated by an intrinsic conduction system consisting of the sinoatrial (SA) node, atrioventricular (AV) node, bundle of His, and Purkinje fibers, all coordinated to generate rhythmic contractions and ensure efficient hemodynamics (Braz *et al.*, 2016). Hemodynamically, Wistar rats exhibit a stroke volume between 0.2 and 0.3 mL and a cardiac output ranging from 60 to 90 mL/min under normal physiological conditions. These values reflect their capacity to maintain systemic circulation through both pulmonary and systemic vascular beds (Damasceno *et al.*, 2013). Their systolic arterial pressure typically measures around 120 mmHg, with diastolic pressure near 80 mmHg, similar to human values when adjusted for size and metabolic rate (Djuric *et al.*, 2020). Regulation of cardiac output in Wistar rats involves both autonomic nervous input and hormonal influences. The sympathetic nervous system enhances cardiac contractility and rate, while parasympathetic input reduces both. The Frank-Starling mechanism also plays a role, whereby increased venous return leads to stronger ventricular contractions. The responsiveness of the rat heart to these regulatory systems has been shown to be comparable to that of larger mammals, enhancing their utility in pharmacological and pathophysiological studies (Chandrasekharan and Elagovan, 2023). Experimental studies involving anesthetics like ketamine and etomidate have

demonstrated that these compounds can significantly modulate hemodynamic parameters such as ventricular contractility and mean arterial pressure, further highlighting the sensitivity of Wistar rat models to cardiovascular perturbations (Djuric *et al.*, 2020). These attributes not only make Wistar rats ideal for modeling human cardiac conditions but also for evaluating the cardiovascular safety profiles of drugs and toxins.

2.3 Malaria-Induced Cardiac Pathology

Malaria, particularly caused by *Plasmodium falciparum*, has traditionally been classified as a hematologic and systemic disease; however, emerging evidence highlights its profound impact on the cardiovascular system, including direct and indirect cardiac pathology. Recent histopathological studies using mammalian models especially Wistar rats and murine systems have shown that *Plasmodium* infection can result in structural and functional heart abnormalities, including myocardial inflammation, vascular congestion, and cardiomyocyte necrosis (Ojha *et al.*, 2021). The pathophysiology of malaria-induced cardiac damage is multifactorial. Sequestration of parasitized erythrocytes in microvascular beds leads to capillary blockage, resulting in ischemic injury and oxidative stress in myocardial tissues (Sarma *et al.*, 2020). This phenomenon, coupled with the systemic inflammatory response, promotes infiltration of mononuclear cells and edema in cardiac interstitium, which has been confirmed in animal histological sections and human autopsies (Gozalo *et al.*, 2024). Further, increased levels of circulating cytokines such as TNF- α , IL-1 β , and IL-6 have been implicated in endothelial activation, promoting thrombosis and impairing coronary perfusion. Cardiac biomarkers such as troponin-I and CK-MB are also elevated during severe infections, indicating cardiomyocyte injury (Pasini and Kocken, 2021). In Wistar rat models infected with *Plasmodium berghei*, studies have reported changes in ventricular wall thickness, diminished ejection fraction, and

interstitial fibrosis, pointing to a progressive form of malaria-related cardiomyopathy (Chukwuochaet *et al.*, 2022). Histologically, malaria-infected cardiac tissues often display disorganization of myofibrils, fragmentation of nuclei, and diffuse hemorrhages. These pathological alterations suggest that in addition to indirect systemic factors such as anemia and hypoxia, the parasite or its byproducts may exert direct cytotoxic effects on cardiac tissues (de Koning-Ward *et al.*, 2016).

2.3.1 Plasmodium falciparum and Myocardial Involvement

Plasmodium falciparum, the most virulent species of the malaria-causing parasites, has historically been associated with severe systemic complications, but recent evidence highlights its capacity to inflict direct and indirect damage on myocardial tissue. Though cardiac manifestations are not classically emphasized in malaria, clinical and experimental studies increasingly show that myocardial involvement is a relevant pathology, especially in severe or cerebral malaria cases. Histopathological studies have revealed several mechanisms of myocardial injury during *P. falciparum* infection. These include microvascular sequestration of infected erythrocytes, cytokine-driven inflammation, oxidative stress, and metabolic acidosis, which together result in ischemic changes and myocardial necrosis. Parasitized red blood cells adhere to vascular endothelium, particularly in capillaries of the heart, leading to impaired perfusion and interstitial edema (Ojha *et al.*, 2021). This microvascular pathology has been reported in both post-mortem human cases and in vivo animal models. Cardiac tissue samples from fatal malaria cases have shown myofibrillar degeneration, mononuclear infiltration, and focal hemorrhage. These histological changes are often accompanied by elevated cardiac enzymes, such as troponin I, CK-MB, and BNP, indicating cardiomyocyte damage (Pasini and Kocken, 2021). Additionally, electrocardiographic abnormalities including prolonged QT

intervals, arrhythmias, and ST-segment changes have been documented, highlighting functional impairment of cardiac conduction during infection. The inflammatory response during *P. falciparum* infection involves a significant release of proinflammatory cytokines like TNF- α , IL-1 β , and IL-6, which contribute to endothelial activation, vascular leakage, and myocardial inflammation. In animal models, these cytokines promote structural disarray in myocardial architecture and mitochondrial dysfunction, often culminating in reduced cardiac output and heart failure symptoms under severe conditions.

2.3.2 Histopathological Changes in the Heart Due to Malaria

Malaria infection, particularly from *Plasmodium falciparum*, leads to distinct histopathological alterations in cardiac tissues, marked by vascular congestion, mononuclear cell infiltration, interstitial edema, and cardiomyocyte degeneration. Recent rodent-based models have provided detailed evidence of these changes. In a study examining malaria drug effects, Wistar rats exhibited mild distortion of cardiac muscle fibers, indicating early myocardial stress even in therapeutic settings (Achilefuet *et al.*, 2023). In post-infection models, histopathology of the myocardium revealed disruption of myocardial architecture, accompanied by hemorrhages and perivascular infiltrates, suggestive of immune-mediated myocardial injury. This parallels findings in infected human tissues, where malaria patients often show focal necrosis, fibrosis, and inflammatory infiltrates within the myocardium (Olatunji *et al.*, 2025).

2.3.4 Myocardial Inflammation and Cardiomyocyte Degeneration

Inflammatory damage in malaria-exposed myocardium is primarily driven by cytokine storms and endothelial dysfunction. Malaria induces elevated TNF- α and IL-6, which promote leukocyte infiltration and microvascular thrombosis, accelerating cardiomyocyte degeneration. Olatunji *et*

al. (2025) emphasized how host–parasite interactions exacerbate myocarditis, marked by interstitial cell infiltration and myofibrillar breakdown . Serum cardiac markers such as AST, CK-MB, LDH, and troponin I were also significantly elevated in experimental malaria infections, correlating with histopathological injury severity (Abdrabouh, 2023). This systemic myocardial response underscores the cardiotoxic potential of parasitemia beyond hematological effects.

2.4 Experimental Models of Malaria in Rodents

2.4.1 Use of Albino Wistar Rats in Malaria Studies

One of the critical advantages of Wistar rats lies in their predictable immune response, which enables controlled modeling of *Plasmodium berghei*-induced malaria, a rodent equivalent to *Plasmodium falciparum* in humans. For example, Totino *et al.* (2019) utilized Wistar rats to demonstrate how eryptosis (programmed red blood cell death) of non-parasitized erythrocytes contributes to severe anemia, even at low parasitemia levels, highlighting parallels with human pathophysiology (Totino *et al.*, 2019). In another study, Jimoh *et al.* (2022) evaluated parasitemia and glucose metabolism in *Plasmodium berghei*-infected diabetic male Wistar rats. Their results confirmed that the co-morbidity model replicates clinically relevant malaria complications, emphasizing the rat's relevance in translational studies (Jimoh *et al.*, 2022). Wistar rats have also been used to explore immunogenic responses to recombinant proteins of *P. falciparum*. Rachmania *et al.* (2021) successfully stimulated CD4⁺ T-cell responses and IgG production against PfEMP1 antigen in Wistar models, reinforcing their validity in vaccine testing frameworks (Rachmania *et al.*, 2021). Moreover, their use in herbal drug research is well documented. Achi *et al.* (2018) administered *Azadirachta indica* leaf extract to malaria-infected Wistar rats and recorded improved survival, reduced parasitemia, and normalized biochemical indices results frequently replicated in phytomedicine investigations (Achi *et al.*, 2018). Ethical

considerations also support their use, as Wistar rats are widely accepted by international animal research standards. They have relatively short gestational periods, high adaptability to lab conditions, and consistent behavior patterns, making them ideal for longitudinal studies involving parasite evolution, immune profiling, and drug resistance mechanisms.

2.4.2 Plasmodium berghei ANKA vs NK65 Strains

The ANKA and NK65 strains of *Plasmodium berghei* are widely utilized rodent models in malaria research due to their genetic tractability and ability to mimic specific aspects of human malaria (SimwelaandWaters, 2022). ANKA strain is most frequently used to study experimental cerebral malaria (ECM) due to its pronounced neurotropic behavior and ability to breach the blood-brain barrier, resulting in neurological complications, brain hemorrhages, and immune cell infiltration (Otunet *et al.*, 2024). In contrast, the NK65 strain is less neurotropic and often preferred in models focusing on systemic inflammation, splenomegaly, and metabolic dysfunction, making it a better option when studying non-cerebral malaria pathogenesis (SimwelaandWaters, 2022). While both strains share basic *P. berghei* characteristics, they differ significantly in immune response elicitation. The ANKA strain stimulates a robust Th1 response, often leading to vascular endothelial damage and cytokine-induced inflammation, particularly in the brain (Goodman *et al.*, 2013). On the other hand, NK65 induces a slower immune progression and is less likely to result in cerebral manifestations, making it advantageous in long-term studies involving chronic malaria and liver pathology (Deroostet *et al.*, 2017). In terms of organ-specific pathology, ANKA is strongly associated with cerebral and pulmonary complications, whereas NK65 demonstrates stronger effects on hepatic injury and splenic architecture distortion (Otunet *et al.*, 2024). Importantly, Simwela and Waters (2022) reported that parasitemia progression is

generally slower in NK65-infected rodents, which may be due to differences in parasite virulence genes and host-pathogen interactions.

2.4.3 Advantages of Wistar Rats for Cardiac Malaria Studies

Wistar rats offer multiple advantages in studying cardiac complications induced by malaria, owing to their physiological similarity to humans, experimental flexibility, and well-characterized baseline cardiac profiles. Their moderate body size and docile temperament make them suitable for invasive procedures such as cardiac puncture, tissue harvesting, and echocardiographic monitoring, all of which are essential in assessing cardiac pathology (Jimoh *et al.*, 2022). Moreover, Wistar rats exhibit a reproducible cardiac response when infected with *Plasmodium berghei*, making them an excellent model for evaluating myocardial inflammation, endothelial dysfunction, and oxidative injury due to malaria infection (Haas *et al.*, 2009). Their vascular structure and electrophysiological characteristics mirror those of humans closely enough to study malaria-induced arrhythmias, ischemia, and hemodynamic imbalance. From a pathophysiological standpoint, Wistar rats enable precise modeling of parasite-induced myocarditis, a growing concern in human malaria. The presence of cardiomyocyte degeneration, vascular congestion, and fibrotic changes in malaria-infected rats allows for histological comparison with postmortem human cardiac tissues (Jimoh *et al.*, 2022). The availability of immunological markers and cardiac enzymes in rat studies also enhances translational research, especially when exploring biomarkers of cardiac damage and cytokine-mediated responses.

2.5 Oxidative Stress and Inflammatory Responses in Malaria

Malaria pathogenesis is strongly influenced by oxidative stress and the resulting inflammatory cascade, both of which contribute to multi-organ damage including the brain and heart. The

infection triggers excessive production of reactive oxygen species (ROS) and reactive nitrogen species (RNS), leading to lipid peroxidation, mitochondrial dysfunction, and DNA damage (Opara *et al.*, 2021). One major source of oxidative stress in malaria is the breakdown of hemoglobin by the parasite, releasing free heme and iron that catalyze the Fenton reaction, generating hydroxyl radicals. Infected red blood cells and phagocytic cells also produce ROS in response to the parasitic load (Adelekan *et al.*, 2020). This pro-oxidative environment overwhelms endogenous antioxidants like glutathione (GSH) and superoxide dismutase (SOD), resulting in cellular apoptosis and inflammation. The inflammatory component is characterized by increased circulating levels of cytokines, particularly tumor necrosis factor-alpha (TNF- α), interleukin-6 (IL-6), and interferon-gamma (IFN- γ). These mediators enhance vascular permeability, endothelial activation, and leukocyte infiltration, processes that contribute to cerebral edema, pulmonary complications, and cardiac inflammation (Jimoh *et al.*, 2022). Malaria-induced inflammation also plays a key role in vascular dysfunction, especially in the brain (leading to cerebral malaria) and myocardium, where cytokines exacerbate microvascular obstruction and ischemic injury. Studies in Wistar rats infected with *Plasmodium berghei* have demonstrated significant increases in malondialdehyde (MDA) and nitric oxide (NO) levels, coupled with declines in antioxidant enzymes hallmarks of oxidative stress-induced pathology (Ogunro *et al.*, 2023).

2.5.1 Malaria-Induced Reactive Oxygen Species (ROS)

The pathogenesis of malaria is intricately linked to the excessive production of reactive oxygen species (ROS), which are generated both by the parasite's metabolism and the host immune response. During the intraerythrocytic cycle, *Plasmodium* species degrade hemoglobin to obtain amino acids, releasing free heme and iron, which in turn catalyze the Fenton reaction to form

hydroxyl radicals, a highly reactive form of ROS (Opara *et al.*, 2021). Additionally, infected erythrocytes produce superoxide radicals and hydrogen peroxide, further contributing to the oxidative burden. Host phagocytes such as macrophages and neutrophils also release ROS as part of the oxidative burst during phagocytosis of infected cells (Adelekan *et al.*, 2020). These reactive species attack lipids, proteins, and nucleic acids, leading to lipid peroxidation, membrane disruption, enzyme inactivation, and DNA fragmentation. In severe cases, this can result in cell death, particularly in highly vascular organs such as the brain, liver, and heart (Jimoh *et al.*, 2022). Elevated ROS levels also activate inflammatory signaling pathways, including NF- κ B and MAPK cascades, promoting the production of TNF- α , IL-1 β , and IL-6. The resulting cytokine storm can cause further oxidative damage and contribute to complications such as cerebral malaria and malaria-induced myocarditis (Ogunroet *et al.*, 2023).

2.5.2 Role of Cytokines in Malaria-Induced Cardiac Damage

Cytokines play a pivotal role in mediating malaria-induced cardiac injury through mechanisms involving systemic inflammation, endothelial activation, and myocardial damage. Proinflammatory cytokines such as tumor necrosis factor-alpha (TNF- α), interleukin-6 (IL-6), interleukin-1 β (IL-1 β), and interferon-gamma (IFN- γ) are released during *Plasmodium* infection and are implicated in cardiac dysfunction. Research has shown that elevated serum levels of TNF- α and IL-6 are associated with increased disease severity and contribute to myocardial inflammation and fibrosis, especially in experimental rodent models of malaria using *Plasmodium berghei* (Popa and Popa, 2021). These cytokines induce endothelial dysfunction, leading to reduced nitric oxide availability, increased vascular permeability, and microvascular congestion, which are key events in malaria cardiopathy (Olanlokunet *et al.*, 2022). IFN- γ and TNF- α also work synergistically to upregulate adhesion molecules (e.g., ICAM-1 and VCAM-

1) on endothelial cells, exacerbating leukocyte adhesion and infiltration into cardiac tissues, resulting in myocardial necrosis and cardiomyocyte apoptosis (de Alba-Alvarado *et al.*, 2024). Moreover, the cytokine storm triggered by severe *Plasmodium falciparum* infection further disrupts the cardiac milieu, with studies showing strong correlation between high IL-6 and TNF- α levels and heart failure markers such as elevated cardiac troponins and CK-MB (Koh *et al.*, 2023). These molecular signatures are often accompanied by reduced cardiac output, a hallmark of malaria-associated myocardial depression (Herr *et al.*, 2011).

2.6 Histopathological Assessment Techniques

Histopathological evaluation remains a cornerstone in understanding the structural and cellular alterations induced by malaria, especially in organ systems such as the heart in rodent models. Several standard and advanced techniques are employed to visualize and quantify pathological changes.

1. Hematoxylin and Eosin (H&E) Staining

H&E staining is the most widely used histological technique due to its ability to clearly delineate tissue architecture. Hematoxylin stains nuclei a deep blue or purple, while eosin stains cytoplasmic and extracellular proteins pink. In malaria studies, H&E is critical for identifying myocardial necrosis, interstitial edema, cardiomyocyte degeneration, and inflammatory infiltrates (Jimoh *et al.*, 2022).

2. Immunohistochemistry (IHC)

IHC allows for antigen-specific localization of proteins within tissues using labeled antibodies. This technique is used to detect proinflammatory cytokines (e.g., TNF- α , IL-6), apoptosis

markers (e.g., caspase-3), or oxidative stress indicators (e.g., 4-HNE, nitrotyrosine) in infected cardiac tissues. IHC provides both spatial and quantitative information, making it superior for mechanistic investigations (Popa and Popa, 2021).

3. Digital Image Analysis

With advancements in microscopy and computing, digital histopathological analysis enables the objective quantification of tissue changes. Image analysis software can measure lesion area, inflammatory cell density, and fibrosis levels, reducing interobserver variability. These tools are increasingly used in malaria pathology studies for standardization and reproducibility (Koh *et al.*, 2023).

4. Special Stains and Markers

In addition to H&E, special stains such as Masson's Trichrome (for fibrosis), Periodic Acid-Schiff (PAS) (for glycogen), and TUNEL assay (for apoptosis) are utilized to reveal specific structural alterations. These techniques provide a more comprehensive evaluation of malaria-induced cardiac damage when used in combination.

2.6.1 Haematoxylin and Eosin (H&E) Staining in Cardiac Tissue

Haematoxylin and Eosin (H&E) staining remains the most widely adopted histological method for evaluating cardiac tissue integrity in rodent models of malaria. The stain combination offers a clear contrast that helps differentiate cellular and extracellular components, allowing researchers to examine tissue architecture, identify degenerative changes, and detect pathological alterations

such as vascular congestion, necrosis, edema, and inflammatory cell infiltration. In malaria-infected rodents, H&E staining is routinely used to assess the severity of myocardial injury. For instance, Achilefuet *et al.* (2023) applied H&E staining in their evaluation of cardiotoxicity in Plasmodium-infected male albino rats treated with dihydroartemisinin-piperaquine, revealing marked inflammation, focal necrosis, and distorted myocardial fibers. Such morphological alterations are common indicators of malaria-associated myocarditis. Maslachahet *et al.* (2020) also utilized H&E staining in histomorphological assessments of cardiac and other vital organs in Plasmodium berghei-infected mice. They noted significant infiltration of mononuclear cells and interstitial edema, which were prominent in untreated and severely infected groups. This supports earlier findings that H&E-stained cardiac tissues can help track the progression of malaria-induced inflammation and necrosis in the heart.

2.6.2 Cardiac Biomarkers in Malaria Pathology

Cardiac biomarkers are increasingly used in malaria studies to evaluate myocardial injury, especially in severe and complicated cases such as cerebral malaria or multi-organ dysfunction. These markers most notably cardiac troponins (TnI and TnT), creatine kinase-MB (CK-MB), B-type natriuretic peptide (BNP), and lactate dehydrogenase (LDH) serve as sensitive indicators of myocardial stress, injury, and inflammation. In malaria-endemic regions, several studies have linked elevated troponin levels with cardiac dysfunction in severe cases. Troponins, especially Troponin I (cTnI), are released into circulation following irreversible myocardial injury, and their presence often correlates with cardiac inflammation or necrosis induced by Plasmodium species (Walker *et al.*, 2020). Similarly, CK-MB, an isoenzyme found primarily in the heart, has been found elevated in rodent models infected with malaria, supporting the role of parasitic infection in triggering cardiomyocyte damage (Oluwatimilehin, 2024). BNP, a hormone secreted

by ventricular cardiomyocytes in response to ventricular stretch and stress, may indicate early-stage heart failure in parasitemic rodents. While it is more extensively studied in human cardiac conditions, its relevance to malaria-induced cardiac stress is being explored as an emerging frontier. Lactate dehydrogenase (LDH), though less specific, remains a reliable marker of generalized cellular injury and metabolic disturbance in malaria (Thirumalasetty, 2024). Elevated LDH in rodent malaria studies suggests widespread tissue hypoxia and hemolysis, indirectly reflecting cardiac strain.

2.7 Comparative Effects of Malaria on Other Organs

Malaria exerts widespread systemic effects, impacting multiple organs beyond the bloodstream. Histopathological studies using rodent models, particularly *Plasmodium berghei*-infected mice, reveal significant structural and functional alterations in vital organs including the liver, kidney, spleen, lungs, and brain.

In the liver, malaria induces congestion, hepatocellular necrosis, and accumulation of malaria pigment (hemozoin), which disrupts hepatic architecture and metabolic function. Okafor *et al.* (2019) observed widespread hepatic necrosis and sinusoidal dilatation in *P. berghei*-infected mice, particularly in groups treated with suboptimal antimalarial therapy, indicating persistent liver injury (Okafor *et al.*, 2019).

Renal pathology is another hallmark of malaria-induced organ damage. Histological changes such as tubular degeneration, glomerular shrinkage, and interstitial hemorrhage have been documented. Maslachahet *al.* (2019) reported nephrotoxic effects marked by tubular epithelial cell damage and proteinaceous casts in kidneys of malaria-infected mice repeatedly exposed to artemisinin (MaslachahandWidiyatno, 2019).

The spleen, being a key immunological filter for blood-borne pathogens, undergoes architectural disorganization, red pulp expansion, and hemosiderosis during infection. Wu and Dayanand (2023) emphasized the immunomodulatory disruption in the spleen, where inflammatory dendritic cells and macrophages accumulate, contributing to dysregulated immune responses (Wu and Dayanand, 2023).

Pulmonary involvement includes alveolar edema, capillary congestion, and inflammatory infiltration, which resemble acute respiratory distress syndrome (ARDS). Histopathological analysis by Maslachah, Suwanti, and Primarizky (2020) revealed extensive lung lesions in infected mice, even in treated groups, indicating the persistence of respiratory inflammation (Maslachah *et al.*, 2020).

The brain, particularly under cerebral malaria conditions, shows hallmark features such as vascular congestion, hemorrhage, neuronal necrosis, and perivascular cuffing. Audu *et al.* (2020) observed intense cerebral pathology in fetal mice born to infected mothers, highlighting the transgenerational impact of malaria on neural tissues (Audu *et al.*, 2020).

2.7.1 Multiorgan Dysfunction Syndrome in Rodent Malaria Models

In Plasmodium-infected mice, the cascade begins with intense proinflammatory cytokine responses, leading to endothelial activation and vascular leakage, which promote tissue hypoxia and immune cell infiltration. This systemic dysregulation results in cumulative damage across multiple organ systems (Nguee *et al.*, 2022).

In the lungs, murine models exhibit acute lung injury (ALI) and acute respiratory distress syndrome (ARDS), marked by alveolar edema, hemorrhage, and inflammatory infiltrates. These

changes correlate with elevated levels of circulating TNF- α and IFN- γ , which compromise alveolar-capillary integrity (Souza *et al.*, 2013).

Renal dysfunction is another hallmark, attributed to immune complex deposition and hemolysis-driven nephrotoxicity. Kidney histology often reveals glomerular atrophy and interstitial inflammation. Katsoulis *et al.* (2021) described how immune-mediated injury, including leukocyte infiltration and endothelial damage, exacerbates acute kidney injury in malaria (Katsoulis *et al.*, 2021).

Cerebral involvement manifests as blood-brain barrier breakdown, neuronal apoptosis, and cerebral edema, especially in experimental cerebral malaria (ECM). Studies have shown that Toll-like receptor (TLR) pathways modulate neuroinflammation and disease severity in ECM (Wu and Dayanand, 2023).

Hepatic pathology includes hepatocyte necrosis, sinusoidal congestion, and Kupffer cell hyperplasia, reflecting both direct parasitic burden and immune-mediated injury. Hepatic dysfunction in malaria is also linked with dysregulated iron metabolism and oxidative stress (de Souza and Pádua, 2016).

Cardiac changes include myocardial degeneration, capillary leakage, and inflammatory cell infiltration. The myocardium, although less commonly studied than other organs, plays a critical role in malaria-induced MODS and contributes to shock and death in advanced stages. (Nguee *et al.*, 2022).

2.8. Antimalarial Agents and Their Cardioprotective Roles

Artemisinin and its derivatives, such as artesunate and dihydroartemisinin (DHA), are reported to protect cardiac tissues by reducing inflammatory mediators and limiting ischemia-induced injury. In a rodent model of myocardial infarction, artesunate significantly reduced infarct size and serum cardiac troponin levels while preserving cardiac architecture (Khan *et al.*, 2018). Similarly, DHA has been shown to suppress NF- κ B activation, leading to downregulation of inflammatory cytokines such as TNF- α and IL-6, which are implicated in malaria-induced myocarditis. Quinine, a traditional alkaloid-based antimalarial, is also recognized for modulating cardiac function. Although it carries a risk of proarrhythmic effects at toxic doses, therapeutic administration can stabilize cardiac output in Plasmodium-infected rodents (Saadeh *et al.*, 2022). Its cardioactivity is believed to be linked with calcium channel modulation and improvement in coronary perfusion under inflammatory stress. Chloroquine, while known for its arrhythmogenic potential at higher concentrations, also exhibits anti-inflammatory and cardioprotective actions when appropriately dosed. A recent pharmacological review noted that chloroquine helps prevent myocardial apoptosis and preserves cardiomyocyte integrity in rodent models challenged with malaria or other systemic inflammatory stimuli (Ain *et al.*, 2024). Moreover, nanotechnology-enhanced delivery systems, such as artemether-loaded polymeric nanocapsules, have been developed to reduce cardiotoxicity while maintaining antiplasmodial potency. These nanoformulations demonstrated significantly lower cardiac tissue damage and improved therapeutic indices in Plasmodium berghei-infected mice compared to conventional artemether (Souza *et al.*, 2018).

2.8.1 Antioxidants and Anti-inflammatory Agents in Malaria Models

Malaria infection triggers excessive production of reactive oxygen species (ROS) through hemolysis, parasite metabolism, and immune responses. These ROS damage cell membranes, mitochondria, and DNA in host tissues. Natural antioxidants such as vitamin C, vitamin E, and polyphenols have demonstrated the capacity to scavenge free radicals, restore redox balance, and reduce lipid peroxidation in malaria-infected rodents (Odeyemi *et al.*, 2021). These agents also mitigate oxidative injury to cardiomyocytes and hepatocytes, preserving tissue integrity. Plant extracts rich in flavonoids and saponins such as those from *Moringa oleifera*, *Curcuma longa* (turmeric), and *Gongronemalatifolium* have shown strong antioxidant and anti-inflammatory properties in experimental *Plasmodium berghei* infections. In a study by Oyeyemi *et al.* (2020), administration of *Gongronemalatifolium* extract to infected rats led to reduced lipid peroxidation and improved histological architecture in both hepatic and renal tissues. Synthetic agents like N-acetylcysteine (NAC) and dexamethasone have also been investigated. NAC replenishes intracellular glutathione levels, protecting against mitochondrial dysfunction in infected mice, while dexamethasone reduces TNF- α , IL-6, and IFN- γ levels, decreasing inflammation-mediated tissue injury (Olorunnisola *et al.*, 2019).

CHAPTER THREE

3.0 MATERIALS AND METHODS

3.1 Study Area

This study was carried out in the experimental site of the Histopathology Laboratory, Department of the University of Benin, Edo State, and the University of Benin Teaching Hospital, Benin City, both in Edo State. Edo State lay between longitude 06°04'E and 06°43'E and latitude 05°44'N and 07°34'N, with a land mass of 17,450 sq. km, located in the south-south geopolitical zone of Nigeria, and with a population of 3.1 million people (World Gazetteer, 2007). The facility provided a controlled environment necessary for experimental infection studies, including standard housing conditions for laboratory animals (temperature 22–26 °C, 12-hour light/dark cycle, and unrestricted access to food and water). The animal house complied with institutional ethical standards and national regulations for the care and use of laboratory animals.

3.2 Collection of Parasite Material

Experimental material, i.e., *Plasmodium berghei* NK65 strain, was obtained from the Nigerian Institute of Medical Research (NIMR). This strain has been widely used as a rodent malaria model due to its close resemblance to human *Plasmodium falciparum* in pathogenesis and disease progression.

3.2.1 Parasite Inoculum Preparation

The inoculum was prepared following the modified method of Ajibola *et al.* (2018). Donor mice previously infected with *Plasmodium berghei* were used to harvest parasitized erythrocytes once parasitemia reached approximately 20–30%. Blood was collected via cardiac puncture into heparinized tubes, then diluted in sterile phosphate-buffered saline (PBS, pH 7.2) to obtain a concentration of 1×10^7 infected red blood cells (iRBCs) per 0.2 mL. This suspension was used for inoculation into experimental rats via intraperitoneal injection.

3.3 Animal Care

Sixteen (16) Adult female albino rats of comparable sizes and weights ranging from 130g to 174g was procured from the animal farm, animal housing facility of the Department of Anatomy, School of Basic Medical Sciences, University of Benin, Benin City. They were acclimatized for two (2) weeks under standard laboratory conditions of 22–26°C temperature. They were kept in wire mesh cages with a tripod that separates the animal from its faeces to prevent contamination. During this period of acclimatization, the rats were fed with Growers' mash and water *ad libitum*. The rats were maintained according to international guidelines for handling experimental animals as reported by the Institute for Laboratory Animal Research (NRC, 1996). The experimental rats were divided into four groups (A – D). Each group contains four rats each (n = 4). Group A served as the positive control, Group B-D served as the test groups.

3.4 Ethical Clearance

Ethical approval for this research was obtained from the Ethics Committee of the Ministry of Agriculture and Natural Resources, Edo State, Nigeria (Approval Number: [V1202/45](#)). All procedures involving animals conformed strictly to the guidelines for the care and use of laboratory animals.

3.5 Experimental Design

The study involved sixteen (16) rats, which were distributed into four groups as follows:

- **Group A (Control):** This group consisted of 4 rats that received only standard feed and water for a duration of forty-two (42) days without any malaria infection.
- **Group B (High Infection Group):** The four (4) rats in this group were infected with high concentrations of *Plasmodium* spp. ($\sim 1 \times 10^6$ parasitized red blood cells) and observed for extended heart pathologies. They also received standard feed and water for a duration of forty-two (42) days.
- **Group C (Medium Infection Group):** The four (4) rats in this group were infected with medium concentrations of *Plasmodium* spp. ($\sim 1 \times 10^4$ parasitized red blood cells) and observed for heart changes. They also received standard feed and water for a duration of forty-two (42) days.
- **Group D (Low Infection Group):** The four (4) rats in this group were infected with low concentrations of *Plasmodium* spp. ($\sim 1 \times 10^2$ parasitized red blood cells) and observed for heart changes. They also received standard feed and water for a duration of forty-two (42) days.
- **2.5 Dosage Calculations**

The therapeutic dose was determined at 10 mg/kg body weight, based on rat body mass.

Formula:

$$X_{\text{mg}} = \frac{(\text{Dose} \times \text{Weight of rat})}{1000} \quad X_{\text{mg}} = 1000(\text{Dose} \times \text{Weight of rat})$$

Example:

For a 140 g rat:

$$X_{\text{mg}} = \frac{(10 \text{ mg} \times 140)}{1000} = 1.4 \text{ mg} \quad X_{\text{mg}} = 1000(10 \text{ mg} \times 140) = 1.4 \text{ mg}$$

The calculated dose was reconstituted in 1 mL sterile distilled water and administered orally via gavage.

3.6 Histopathological Analysis

At the end of the 42-day experimental period, four (4) rats per group were humanely euthanized via cervical dislocation. The hearts were harvested, rinsed in ice-cold saline, and fixed in 10% neutral buffered formalin (NBF) for 24 hours.

3.6.1 Processing of Histology Sample

At the end of the experiment, four (4) rat from each group were humanely euthanized via cervical dislocation, 24 hours after last day of administration. The hearts tissues were harvested for Groups A,B,C and D for the experiment using sterile surgical blade. The dissected hearts tissues were examined for ulceration or inflammation (Bancroft *et al.*, 2019).

3.6.2 Histological Technique

Procedure:

Histopathologically, to detect inflammation, the whole organ (that is the hearts tissues) were autopsied, stained using hematoxylin and eosin staining techniques to demonstrate general tissue structure and then viewed microscopically. The procedure involved includes:

TISSUE (The hearts tissues) processing using automatic method. Sequences for automatic tissue processing were as follows:

Harvesting Tissue: The required tissues (hearts tissues) were harvested from the rats and immediately put in a fixative. All parts of the required tissue that showed obvious microscopic changes were essentially selected for sampling. Tissues were cut into thin slices of 3mm by size.

For histological evaluation, the heart was selected due to its central role in circulation, oxygen delivery, and metabolic homeostasis, as well as its susceptibility to pathological alterations induced by infectious, toxicological, or ischemic insults. The heart, a muscular organ located in the mediastinum, is responsible for maintaining systemic and pulmonary blood flow through rhythmic contractions. Structurally, it is composed of three primary layers: the **endocardium**, **myocardium**, and **epicardium**. The myocardium, consisting of branching cardiac muscle fibers with centrally located nuclei and intercalated discs, serves as the contractile component and is a critical indicator of myocardial health. Pathological evaluation of cardiomyocytes can reveal necrosis, hypertrophy, cytoplasmic vacuolation, and nuclear pyknosis, which are hallmarks of cardiotoxicity and infectious damage (Ross & Pawlina, 2016). Cardiac interstitial tissue contains fibroblasts, vascular elements, and inflammatory cells that provide additional markers of pathological responses such as edema, fibrosis, or infiltration by immune cells. The coronary vasculature, vital for myocardial oxygenation, is also an important histological marker, as vascular congestion, endothelial swelling, and hemorrhage frequently accompany cardiac injury.

The **endocardium**, which lines the cardiac chambers, and the **epicardium**, containing connective tissue and mesothelial cells, can also exhibit pathological thickening, inflammatory infiltration, or degenerative changes in disease states. Following collection, the heart tissues were fixed in **10% neutral buffered formalin (NBF)**, prepared from commercial formalin (37–40% formaldehyde), sodium dihydrogen phosphate monohydrate, disodium hydrogen phosphate anhydrous, and tap water, maintaining a neutral pH of ~7.0 to prevent formalin pigment formation and ensure morphological preservation (Bancroft & Gamble, 2008). Tissues were immersed in NBF for at least 24 hours at room temperature to achieve thorough penetration and stabilization of myocardial architecture, preventing autolysis and minimizing artifacts. After fixation, dehydration was carried out by sequential immersion in graded alcohols (70%, 90%, and 95% ethanol), followed by three rounds of absolute alcohol, each lasting 2 hours and using a volume 50–100 times the tissue volume. The samples were then cleared in two changes of xylene for 90 minutes each, removing residual alcohol and preparing the myocardium for paraffin infiltration. Paraffin wax impregnation was performed at wax melting temperature, using tissue-to-wax ratios of 1:25–30, with two changes of molten wax, each lasting 2 hours, to ensure complete infiltration of myocardial fibers and vascular structures. Finally, the heart tissues were embedded in labeled cassettes with molten paraffin wax, solidified, and cooled rapidly in cold water. The hardened blocks were trimmed and sectioned at 4–5 μm thickness using a digital rotary microtome (Histoline MR3000, Italy). Sections were mounted on clean, grease-free slides and subjected to hematoxylin and eosin (H&E) staining, enabling detailed evaluation of cardiomyocyte architecture, intercalated discs, vascular patterns, and pathological alterations indicative of *Plasmodium*-induced or toxicological cardiac injury.

Staining of Processed Tissues

Tissue sections prepared for general histological evaluation were stained using the Ehrlich's Haematoxylin and Eosin (HandE) staining technique, following the method outlined by Archibong *et al.* (2021).

Principle: Hematoxylin is a basic dye and thus has affinity for the acidic part of the cellular component which is the nucleus. Therefore, the nucleus stains blue while eosin on the other hand is an acidic dye thus has affinity for the basic component of the cells which is the cytoplasm therefore it stains it pink which is the color of the dye. This staining procedure was facilitated with a mordant that linked the stain to the tissue and a differentiator (acid alcohol) that differentiated the nuclear stain from cytoplasmic stain.

Procedure For Hematoxylin And Eosin Staining

Tissue sections were initially dewaxed by immersing them in two changes of xylene, each for 2 minutes, to remove paraffin wax. This was followed by rehydration through a descending alcohol series, starting with absolute alcohol for 2 minutes, then 90% alcohol for 1 minute, and finally 70% alcohol for 1 minute. The slides were then rinsed under running tap water for 1 minute to remove residual alcohol. After rehydration, the sections were stained with hematoxylin for 10 minutes to highlight nuclear structures. Excess stain was removed by brief rinsing in distilled water for 30 seconds, followed by differentiation in 1% acid alcohol for 15 seconds to enhance contrast. The slides were then rinsed thoroughly in distilled water for 5 minutes to stop the differentiation process. Subsequently, the tissues were counterstained with 1% eosin for 5 minutes to visualize cytoplasmic and extracellular components. After staining, the sections were rinsed in running tap water for 30 seconds, then dehydrated through ascending grades of alcohol 70%, 90%, and 100% for 1 minute each. Dehydrated slides were cleared in two changes of

xylene for 2 minutes each to remove alcohol and make the tissue transparent. Finally, the sections were mounted using DPX mounting medium and examined microscopically under an objective lens to assess histological features (Archibong *et al.*, 2021).

3.6.3 Microscopy And Photomicrography

Tissue sections were examined at 40× and 100× magnifications using an Olympus CX23 binocular light microscope, equipped with an integrated LED illumination system to ensure consistent and high-contrast visualization of histological features. For image documentation, photomicrographs were captured using an Olympus BX53 trinocular microscope fitted with an Olympus DP74 high-resolution digital camera. The setup was connected to a computer via Olympus cellSens imaging software, which facilitated accurate acquisition and processing of the microscopic images.

3.6.4 Statistical Analysis

The mean and standard deviation were used to express all weight results. Statistical programs for Social Sciences (SPSS) version 20 was used to conduct the statistical analysis on the mean weight of the heart, initial body weight to final body weight of the rat.

CHAPTER FOUR

RESULTS

4.1 Histopathological Changes

The following are the histological findings observed in the course of investigating the Heart tissue after administering different doses of *Plasmodium berghei* (Group A= control, Group B=high concentrations of *Plasmodium* spp. ($\sim 1 \times 10^6$ parasitized red blood cells), Group C= medium concentrations of *Plasmodium* spp. ($\sim 1 \times 10^4$ parasitized red blood cells), Group D= low concentrations of *Plasmodium* spp. ($\sim 1 \times 10^2$ parasitized red blood cells):

4.1.1 Heart

Section of cardiac muscle from control rats revealed myocytes (arrow) with peripherally placed nuclei surrounded by abundant eosinophilic cytoplasm. The muscle fibers appeared long, cylindrical, and striated, arranged in parallel bundles with clear intercalated discs demarcating adjacent cells. No evidence of necrosis, vacuolation, inflammatory infiltration, or fibrotic changes was observed (**Plate 4.1A**).

Section of cardiac muscle from rats administered high concentrations of *Plasmodium* spp. ($\sim 1 \times 10^6$ parasitized red blood cells) revealed myocytes (arrow) with peripherally placed nuclei surrounded by abundant eosinophilic cytoplasm. The cardiac fibers appeared long, cylindrical, and striated, with intact intercalated discs demarcating adjacent cells. No evidence of vacuolation, necrosis, inflammatory infiltration, or fibrosis was observed (**Plate 4.1B**).

Section of cardiac muscle from rats administered medium concentrations of *Plasmodium* spp. ($\sim 1 \times 10^4$ parasitized red blood cells) revealed myocytes (arrow) with peripherally placed nuclei

surrounded by eosinophilic cytoplasm. The cardiac fibers retained their normal striated pattern and cylindrical morphology with intact intercalated discs. No evidence of cytoplasmic vacuolation, degeneration, necrosis, or inflammatory cell infiltration was observed (Plate 4.1C).

Section of cardiac muscle from rats administered low concentrations of *Plasmodium* spp. ($\sim 1 \times 10^2$ parasitized red blood cells) revealed myocytes (arrow) with peripherally placed nuclei surrounded by eosinophilic cytoplasm. The myocardial fibers appeared elongated, striated, and well-organized with intact intercalated discs. No evidence of cytoplasmic vacuolation, necrosis, degeneration, or inflammatory infiltration was noted (**Plate 4.1D**).

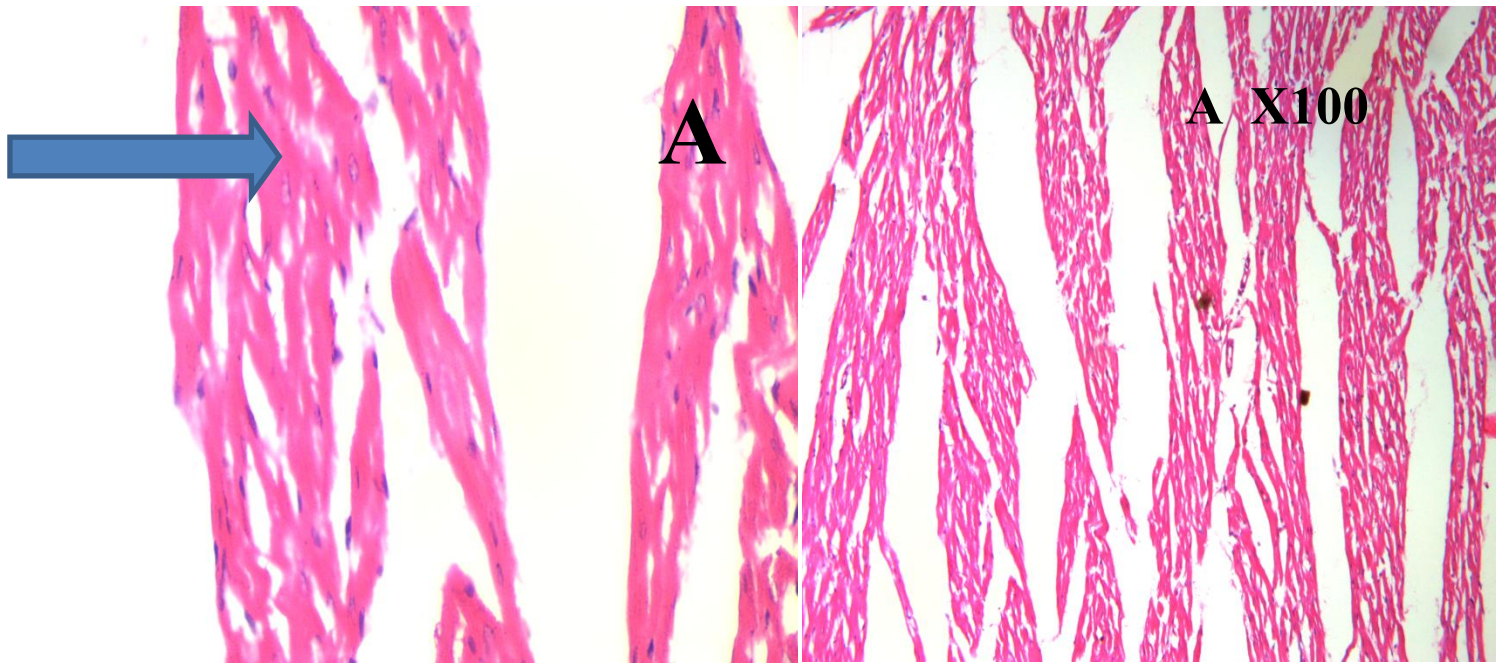


Plate 4.1A: Section of cardiac muscle from control rats revealed myocytes (arrow) with peripherally placed nuclei surrounded by eosinophilic cytoplasm. Features are in keeping with NORMAL MYOCYTESH and E Mag x400

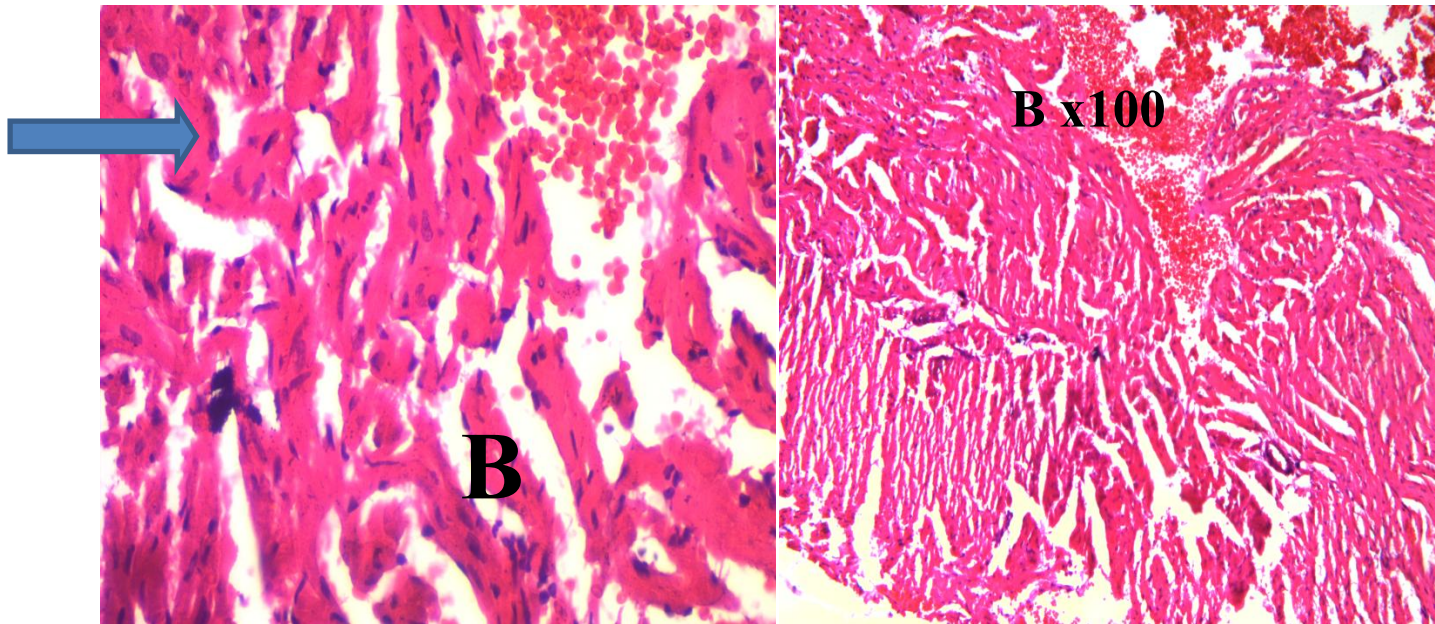


Plate 4.1B: Section of cardiac muscle from rats administered high concentrations of *Plasmodium* spp. ($\sim 1 \times 10^6$ parasitized red blood cells) revealed myocytes (arrow) with peripherally placed nuclei surrounded by eosinophilic cytoplasm. Features are in keeping with NORMAL MYOCYTES H and E Mag x400

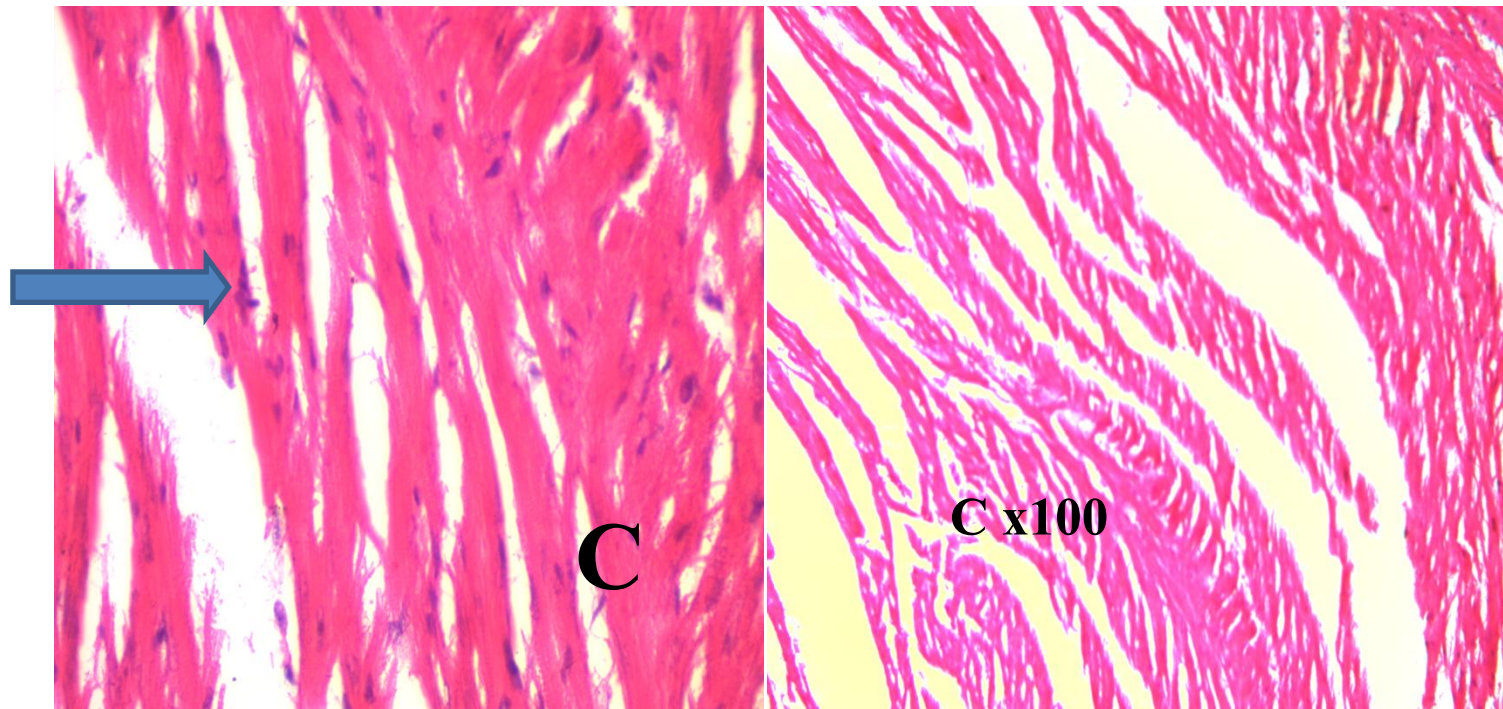


Plate 4.1C: Section of cardiac muscle from rats administered medium concentrations of *Plasmodium* spp. ($\sim 1 \times 10^4$ parasitized red blood cells)myocytes (arrow) with peripherally placed nuclei surrounded by eosinophilic cytoplasm. Features are in keeping with NORMAL MYOCYTES H and E Mag x400

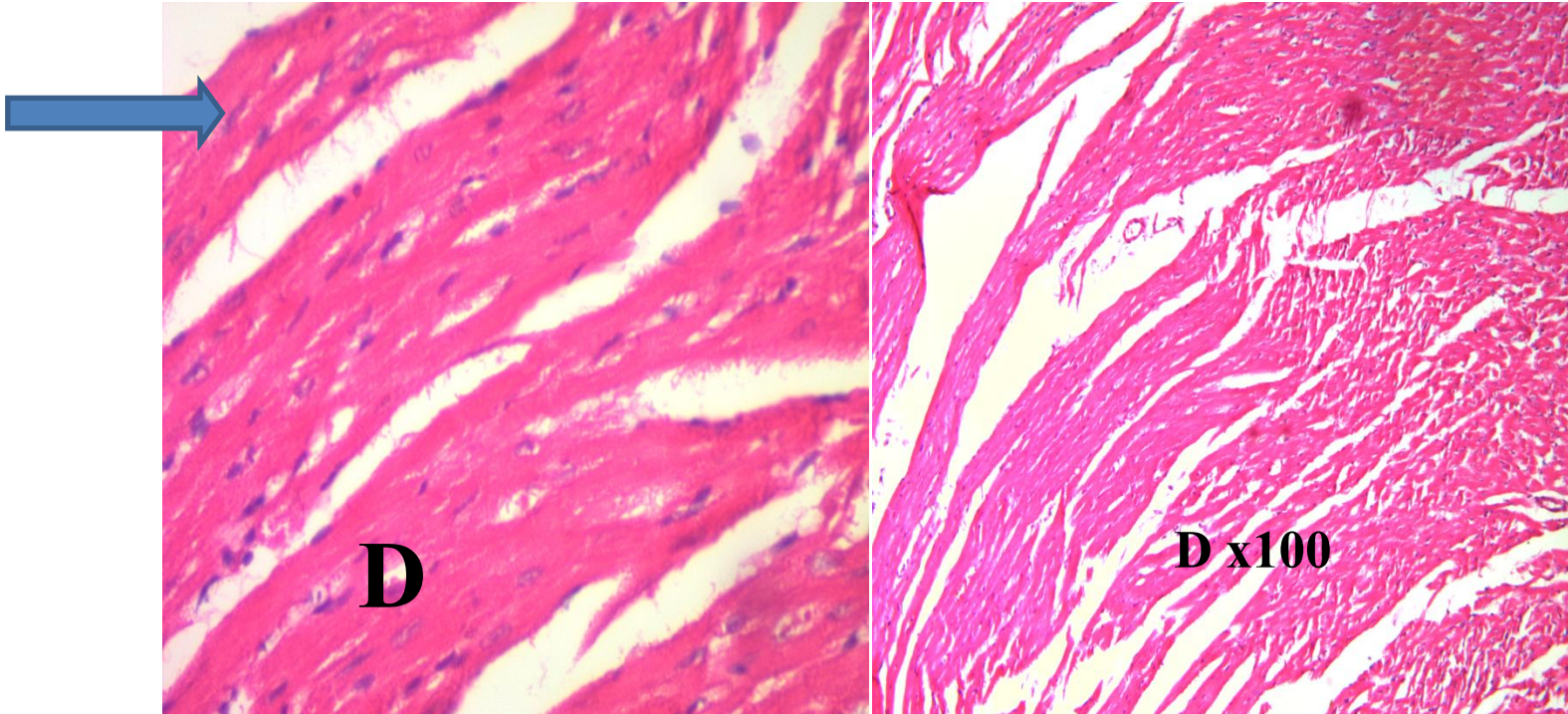


Plate 4.1D: Section of cardiac muscle from rats administered low concentrations of *Plasmodium* spp. ($\sim 1 \times 10^2$ parasitized red blood cells) myocytes (arrow) with peripherally placed nuclei surrounded by eosinophilic cytoplasm. Features are in keeping with NORMAL MYOCYTES H and E Mag x400

As shown in **Table 4.1**, no significant differences were observed in initial body weight ($p = .706$), final body weight ($p = .553$), or heart weight ($p = .939$) across the experimental groups. This is also demonstrated in **Figure 4.1** (initial weight), **Figure 4.2** (final weight), and **Figure 4.3** (heart weight), all of which indicate no statistically significant variation between groups. For final body weight, the absence of significant differences ($p = 0.553$) suggests that the Malaria Parasite did not markedly alter the growth or overall health status of the animals over the experimental period. While Group B (high dose) showed a numerically lower mean final weight (129.8 ± 2.29 g) compared to the control (143.0 ± 6.01 g), the variation was within the margin of biological variability and did not reach statistical significance. This implies that the treatment, even at the highest dose, did not cause weight loss severe enough to be considered toxicologically relevant. Similarly, the analysis of heart weight showed no significant differences between groups ($p = 0.939$). This finding indicates that the treatment did not exert any cardiotoxic effect or result in hypertrophy/atrophy of cardiac tissue. The consistency in heart weight across groups further supports the safety profile of the test substance with respect to cardiac morphology.

Table 4.1. Body and Organ Weights

Parameter	Group A (control)	Group B (Hgh dose)	Group C (Middle dose)	Group D (low dose)	p-value
Initial Weight (g)	142.0 ± 7.14	135.5 ± 3.97	145.8 ± 9.63	145.5 ± 5.72	0.706
Final Weight (g)	143.0 ± 6.01	129.8 ± 2.29	138.3 ± 9.96	139.5 ± 5.66	0.553
Heart Weight (g)	0.65 ± 0.06	0.63 ± 0.03	0.65 ± 0.09	0.60 ± 0.07	0.939

Values are Mean ± SEM (n=4 per group). *Significant differences indicated at p<0.05.*

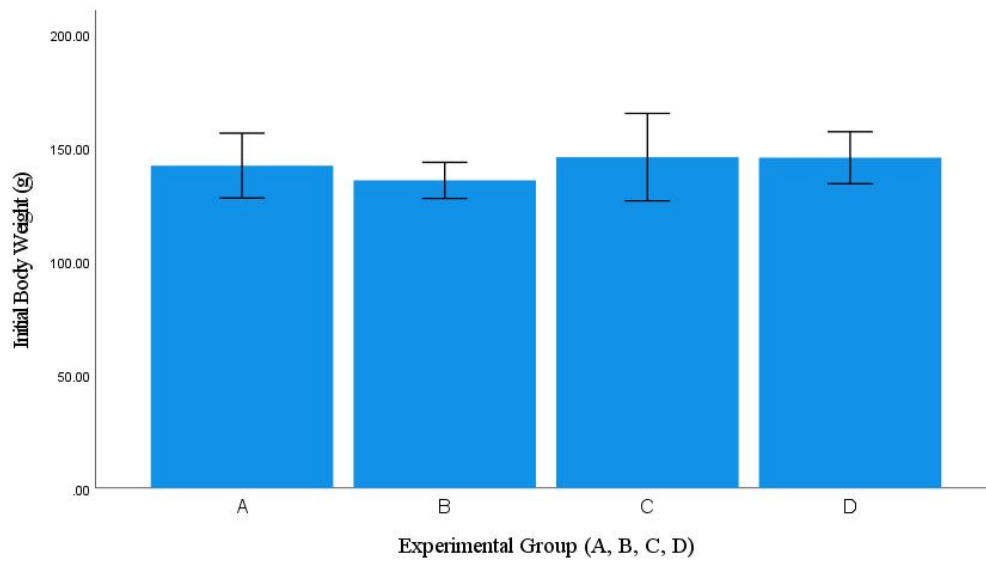


Figure 4.1. Initial body weight no statistical significance between groups $p = 0.706$)

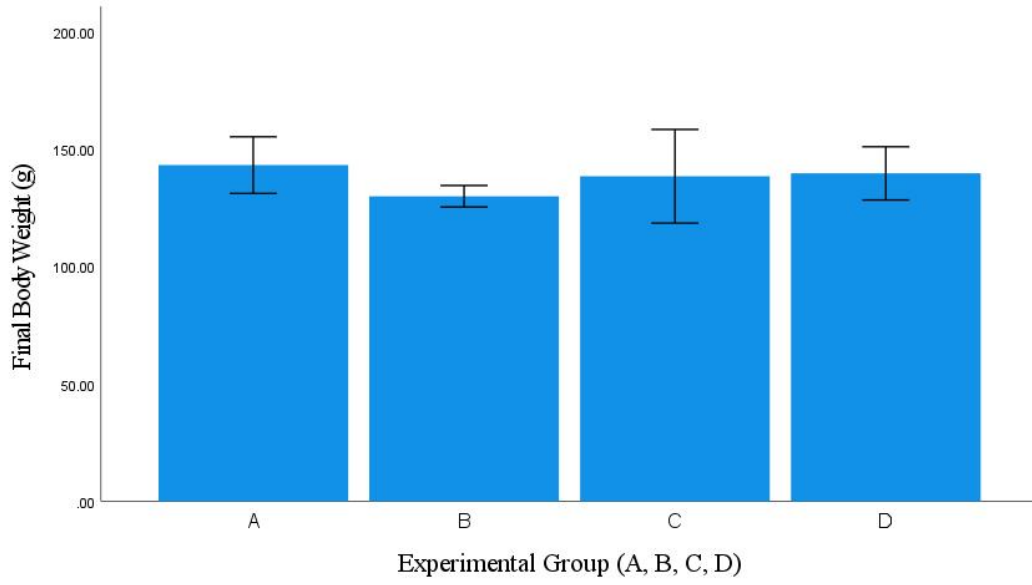


Figure 4. 2. Final body weight, no statistical significance between groups $p = 0.553$

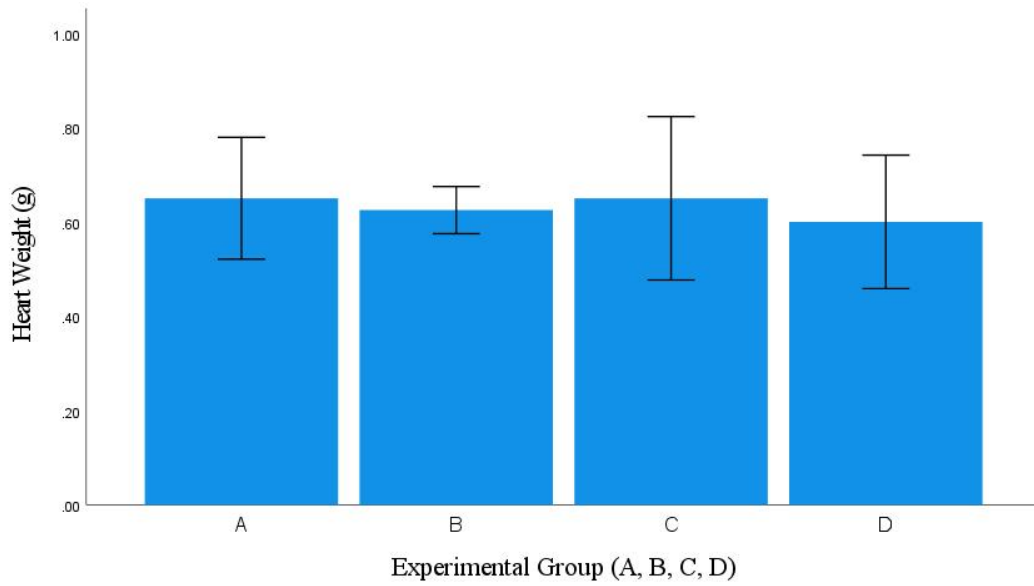


Figure 4. 3. Heart weight, no statistical significance between groups $p = 0.939$

CHAPTER FIVE

DISCUSSION AND CONCLUSION

5.1 Discussion

The present study evaluated the histopathological and morphometric effects of *Plasmodium berghei* infection on cardiac tissues of Wistar rats exposed to varying concentrations of parasitized red blood cells (PRBCs). Across all treatment groups — low ($\sim 1 \times 10^2$ PRBCs), medium ($\sim 1 \times 10^4$ PRBCs), and high ($\sim 1 \times 10^6$ PRBCs) — myocardial histoarchitecture remained largely preserved and comparable to the control group. Cardiac myocytes demonstrated characteristic features of normal morphology, including peripherally placed nuclei, eosinophilic cytoplasm, elongated and striated fibers, and intact intercalated discs. Importantly, no evidence of necrosis, vacuolation, fibrosis, inflammatory infiltration, or architectural distortion was observed, suggesting that the parasite load, within the experimental timeframe, did not induce overt cardiotoxic or pathological effects.

The lack of pathological changes in the myocardium in this study contrasts with several reports that describe malaria as a systemic disease capable of involving the heart. For instance, *Silva et al.* (2013) observed interstitial edema, myocyte degeneration, and inflammatory infiltrates in mice infected with *Plasmodium chabaudi*, while *Sanyaolu et al.* (2019) highlighted the potential of *Plasmodium falciparum* infection to cause myocarditis and arrhythmias in human cases. Similarly, *Parroche et al.* (2007) demonstrated immune-mediated damage in malaria infections, where pro-inflammatory cytokines and oxidative stress contributed to myocardial injury. In contrast, the present findings are consistent with reports indicating that acute or early malaria infection may not produce visible histopathological cardiac lesions. *Pongponratn et al.* (2012)

noted that acute malaria predominantly affects microvasculature and systemic organs such as the liver and spleen, with the myocardium often spared in the early stages. This aligns with our findings, which showed intact myocyte morphology across low, medium, and high parasite concentrations.

The analysis of initial and final body weights revealed no statistically significant differences across the experimental groups ($p = 0.706$ and $p = 0.553$, respectively). Although rats in the high-dose group (1×10^6 PRBCs) exhibited a numerically lower mean final weight (129.8 ± 2.29 g) compared to controls (143.0 ± 6.01 g), the difference did not reach statistical significance. This suggests that malaria parasitemia, even at high levels, did not substantially alter growth or induce weight loss within the study duration. These results contrast with findings from *Franke-Fayard et al. (2006)* and *Craig et al. (2012)*, who reported weight loss and reduced survival in rodent malaria models, typically attributed to parasitemia-induced anorexia, metabolic derangements, and systemic inflammation. The discrepancy may be explained by differences in infection duration, host strain susceptibility, or parasite strain virulence. Our findings instead align with *Iyawe et al. (2017)*, who observed that short-term infections or subclinical parasitemia may not markedly affect host growth metrics.

Similarly, heart weights across all groups remained comparable ($p = 0.939$), indicating no cardiomegaly, atrophy, or significant tissue remodeling occurred in response to parasite challenge. This absence of myocardial hypertrophy or atrophy supports the notion that acute infection did not exert sufficient stress to alter cardiac morphology. Comparable results were reported by *Otto et al. (2018)*, who showed that detectable structural cardiac changes in malaria are often secondary to severe or chronic infections, particularly when associated with systemic

complications such as anemia, hypoxia, or high inflammatory burden. The preservation of myocardial histoarchitecture across parasite doses suggests a degree of resilience of the cardiac tissue in the early stages of *P. berghei* infection. However, it is important to note that histology alone may not fully capture subtle molecular or functional changes. Previous studies have shown that malaria can induce oxidative stress, mitochondrial dysfunction, and electrophysiological abnormalities that precede visible histopathological alterations. For example, *Guha et al.* (2014) demonstrated malaria-associated oxidative stress in cardiomyocytes, while *Anigbo et al.* (2020) reported conduction abnormalities in malaria-infected models without overt structural damage.

Thus, while our findings indicate no structural cardiac pathology, it remains possible that subcellular or biochemical derangements were present but undetectable using routine hematoxylin and eosin (H&E) staining. In human malaria, particularly with *P. falciparum* infection, cardiac complications such as myocarditis, pericarditis, arrhythmias, and even heart failure have been documented (*Ehrhardt et al., 2004; Joshi et al., 2017*). These manifestations are often linked to cytoadherence of parasitized erythrocytes, microvascular obstruction, and intense systemic inflammation. The absence of such changes in this experimental study may reflect differences between rodent and human malaria pathophysiology, with *P. berghei* in rodents not entirely replicating the severe microvascular pathology of *P. falciparum* in humans.

Taken together, this study demonstrates that within the short experimental duration, infection with *P. berghei* at low, medium, and high parasitic loads does not result in significant histopathological or morphometric alterations in the heart of Wistar rats. The results highlight an apparent limitation of rodent malaria models in fully capturing the cardiac complications observed in human malaria. They also emphasize the importance of complementing

histopathological evaluation with molecular, biochemical, and electrophysiological analyses to provide a more comprehensive understanding of malaria-induced cardiotoxicity.

5.2 Conclusion

The present study investigated the histopathological and morphometric effects of *Plasmodium berghei* infection on the heart of Wistar rats at varying concentrations of parasitized red blood cells. The findings revealed that across all doses tested — low ($\sim 1 \times 10^2$ PRBCs), medium ($\sim 1 \times 10^4$ PRBCs), and high ($\sim 1 \times 10^6$ PRBCs) — cardiac myocytes retained their normal morphology, characterized by peripherally placed nuclei, abundant eosinophilic cytoplasm, intact striations, and well-preserved intercalated discs. No evidence of necrosis, vacuolation, fibrosis, or inflammatory infiltration was observed, indicating that the parasite burden did not induce overt structural myocardial damage within the experimental timeframe. Furthermore, body weights, final weights, and heart weights remained statistically comparable across all groups, demonstrating that *P. berghei* infection, under the conditions studied, did not adversely affect overall growth or cardiac organ mass. These results suggest that in the acute phase, *P. berghei* infection may not significantly compromise cardiac architecture or weight, highlighting a degree of resilience in myocardial tissue against early parasitemia.

5.3 Recommendations

Based on the findings of this study, it is recommended that future investigations extend beyond histopathological assessments to include biochemical and molecular analyses, such as cardiac enzyme profiling (e.g., troponins, creatine kinase-MB) and markers of oxidative stress, which may reveal subclinical myocardial damage not evident under light microscopy. Advanced techniques such as immunohistochemistry, electron microscopy, and echocardiography are also

suggested to evaluate ultrastructural and functional cardiac alterations associated with malaria infection. Secondly, the study duration should be extended to capture the chronic phase of infection, as myocardial complications of malaria may manifest over a longer time course. Dose–response studies with higher parasitemia levels and repeated infections are also warranted to better mimic clinical malaria progression in humans. Thirdly, it is recommended that future research include comparative studies across Plasmodium species, given the variability in pathogenicity and systemic involvement between *P. berghei*, *P. falciparum*, and *P. vivax*. Such comparisons would provide more translational insights into human malaria cardiopathology. Finally, since malaria is often associated with systemic complications, it is advisable to investigate the interplay between cardiac changes and other organ systems (e.g., liver, kidney, spleen) to establish a comprehensive picture of malaria-induced multi-organ pathology. This will also facilitate the development of targeted therapeutic and prophylactic interventions aimed at minimizing cardiac complications in malaria-endemic populations.

REFERENCES

- Abdrabouh, A. E. S. (2023). Toxicological and histopathological alterations in the heart of young and adult albino rats exposed to mosquito coil smoke. *Environmental Science and Pollution Research*, 30(27)171694–71708.
- Achilefu, R. C., Jumbo, U. K., & Oti, D. C. (2023). Histopathological evaluation of the cardiotoxicity of dihydroartemisinin-piperaquine on male albino rats. *Journal of Biosciences and Medicines*, 11(12):1–10.
- Adelekan, A. O., Oyewo, E. B., & Ajani, E. O. (2020). Antioxidant status and lipid peroxidation in *Plasmodium berghei*-infected mice treated with *Morinda lucida* extract. *African Journal of Infectious Diseases*, 14(2):37–45.
- Adeyemo, F. O., Akinyemi, A. J., & Ajayi, I. O. (2022). Protective role of vitamin C in malaria-induced organ damage in *Plasmodium berghei*-infected mice. *Journal of Functional Foods*, 98(2):105290.
- Ahmed, M. Z., Sharma, S., Bhardwaj, N., & Srivastava, B. (2020). Clinicopathological study of potential biomarkers of *Plasmodium falciparum* malaria severity and complications. *Infection, Genetics and Evolution*, 85: 104512.
- Ain, Q. T., Saleem, N., Munawar, N., & Nawaz, R. (2024). Quest for malaria management using natural remedies. *Frontiers in Pharmacology*, 15:1359890.
- Aly, A. S. I., Vaughan, A. M., & Kappe, S. H. I. (2009). Malaria parasite development in the mosquito and infection of the mammalian host. *Annual Review of Microbiology*, 63, 195–221.
- Aminu, M. A., Ur Rehman, A., & Azizan, N. A. (2024). Malaria and cardiometabolic health: A review of its impact on metabolic and cardiovascular disorders. *Malaysian Journal of Medicine and Health Sciences*, 20(2):–72.

- Anigbo, C. J., Ezeani, C. C., &Uchegbu, R. I. (2020). Malaria-induced cardiac conduction abnormalities: Insights from experimental models. *Journal of Parasitic Diseases*, 44(3):543–550.
- Audu, D., Idowu, A. B., Idowu, O. A., &Mshelbwala, F. M. (2020). Haematological alteration and histopathology of vital organs of pups delivered by mice infected with *Plasmodium berghei* during the second and third stage of pregnancy. *Animal Research International*, 17(2):3716–3727.
- Behera, P. K., Mishra, S. K., &Satpathi, S. (2013). Cardiac involvement in malaria: An overlooked important complication. *Journal of Vector Borne Diseases*, 50(3):232–235.
- Brainin, P., Gomes, L. C., Holm, A. E., & Matos, L. O. (2023). Left ventricular function by strain in uncomplicated malaria: A prospective study from the Brazilian Amazon. *The International Journal of Cardiovascular Imaging*, 39(1):91–103.
- Brainin, P., Gomes, L. C., Holm, A. E., & Matos, L. O. (2023). Left ventricular function by strain in uncomplicated malaria: A prospective study from the Brazilian Amazon. *The International Journal of Cardiovascular Imaging*, 39(1):91–103.
- Brainin, P., Mohr, G. H., Modin, D., Claggett, B., et al. (2021). Heart failure associated with imported malaria: A nationwide Danish cohort study. *ESC Heart Failure*, 8(6):5336–5345.
- Braz, G. R. F., Pedroza, A. A., & Nogueira, V. O. (2016). Serotonin modulation in neonatal age does not impair cardiovascular physiology in adult female rats: Hemodynamics and oxidative stress analysis. *Life Sciences*, 166: 51–58.
- Cardim, N., &Barberato, S. H. (2025). Cardiovascular imaging in tropical infectious myocarditis: Insights from malaria. *European Heart Journal - Cardiovascular Imaging*.
- Carvalho, C. A. M., &Thomazini, J. A. (2013). Morphometric and anatomical evaluation of the heart of Wistar rats. *International Journal of Morphology*, 31(2):470–476.
- Chandrasekharan, A. B., & Elagovan, B. (2023). Albino Wistar rat models in cardiovascular disease research. *Cardiovascular Research*.

- Chukwuocha, U. M., Amah, C. C., & Okeke, N. J. (2022). Histopathological alterations in the myocardium of albino rats infected with *Plasmodium berghei*. *Nigerian Journal of Parasitology*, 43(1):56–61.
- Craig, A. G., Grau, G. E., Janse, C., Kazura, J. W., Milner, D., Barnwell, J. W., & Turner, G. (2012). The role of animal models for research on severe malaria. *PLoS Pathogens*, 8(2):2401.
- Damasceno, D. D., Lima, M. P., Motta, D. F., & Ferreira, A. J. (2013). Cardiovascular and electrocardiographic parameters after tonin administration in Wistar rats. *Peptides*, 42: 95–101.
- de Alba-Alvarado, M. C., Cabrera-Bravo, M., & Zenteno, E. (2024). The functions of cytokines in the cardiac immunopathogenesis of Chagas disease. *Pathogens*, 13(10): 870.
- De Carvalho, C. A. M., & Thomazini, J. A. (2014). Study of Wistar rats' heart at different stages in the evolutionary cycle. *International Journal of Morphology*, 32(3): 820–826. PDF
- de Koning-Ward, T. F., Dixon, M. W. A., & Tilley, L. (2016). *Plasmodium* species: master renovators of their host cells. *Nature Reviews Microbiology*, 14(8), 494–507.
- De Russi, B. M., & Carvalho, C. A. M. (2019). Anatomic and embryological aspects of the cardiovascular system of albino Wistar rats. *Thieme Connect*.
- de Souza, M. C., & Pádua, T. A. (2016). Multiple organ dysfunction during severe malaria: The role of the inflammatory response. In *Experimental Models of Malaria* (pp. 85–100).
- Deroost, K., Corbett, Y., Lays, N., & Corsetto, P. (2017). Differential induction of malaria liver pathology in mice infected with *Plasmodium chabaudi* AS or *Plasmodium berghei* NK65. *Malaria Journal*, 16(1):2159.
- Djokic, V., Rocha, S. C., & Parveen, N. (2021). Lessons learned for pathogenesis, immunology, and disease of erythrocytic parasites: *Plasmodium* and *Babesia*. *Frontiers in Cellular and Infection Microbiology*, 11: 685239.

- Djuric, M., Kostic, S., Nikolic Turnic, T., & Stankovic, S. (2020). The comparison of the effects of ketamine and etomidate on cardiodynamics, biochemical and oxidative stress parameters in Wistar male rats. *Molecular and Cellular Biochemistry*, 473(2):91–99.
- Dow, G. S., Armson, A., Boddy, M. R., & Itenge, T. (2002). *Plasmodium*: Assessment of the antimalarial potential of trifluralin and related compounds using a rat model of malaria (*Rattus norvegicus*). *Experimental Parasitology*, 100(1):43–51.
- Ehrhardt, S., Wichmann, D., Hemmer, C. J., Burchard, G. D., & Brattig, N. W. (2004). Circulatory and cardiac manifestations of falciparum malaria: A review. *American Journal of Tropical Medicine and Hygiene*, 71(5):753–760.
- Farina, J. M., Gupta, S., Gazendam, N., Saldarriaga, C., & Briel, M. (2021). Malaria and the heart: JACC state-of-the-art review. *Journal of the American College of Cardiology*, 77(10):1247–1265.
- Farina, J. M., Liblik, K., & Iomini, P. (2023). Infections and cardiovascular disease: JACC Focus Seminar 1/4. *Journal of the American College of Cardiology*, 81(9):1022–1038.
- Fikadu, M., & Ashenafi, E. (2023). Malaria: an overview. *Infection and Drug Resistance*, 16(1):587–596.
- Franke-Fayard, B., Janse, C. J., Cunha-Rodrigues, M., Ramesar, J., Büscher, P., Que, I., ... Waters, A. P. (2006). Murine malaria parasite sequestration: CD36 is the major receptor, but cerebral pathology is unaltered. *Proceedings of the National Academy of Sciences*, 103(36):13120–13125.
- Gomes, L. C., Marinho, C. R. F., & Holm, A. E. (2021). Prevalence of cardiovascular complications in malaria: A systematic review and meta-analysis. *The American Journal of Tropical Medicine and Hygiene*, 104(5), 1782–1790.
- Goodman, A. L., Forbes, E. K., Williams, A. R., & Douglas, A. D. (2013). The utility of *Plasmodium berghei* as a rodent model for anti-merozoite malaria vaccine assessment. *Scientific Reports*, 3(1706).

- Gozalo, A. S., Robinson, C. K., & Holdridge, J. (2024). Overview of *Plasmodium* spp. and animal models in malaria research. *Comparative Medicine*, 74(4), 301–312.
- Guha, M., Kumar, S., Choubey, V., Maity, P., & Bandyopadhyay, U. (2014). Apoptosis in liver during malaria: Role of oxidative stress and implications for therapy. *Journal of Biosciences*, 39(3):531–544.
- Gupta, S., Gazendam, N., Farina, J. M., Saldarriaga, C., & Briel, M. (2021). Pathophysiological link between Plasmodium infection and cardiovascular disease: Emerging insights. *JACC Review Topic of the Week*, 77(10):1247–1265.
- Haas, S. E., Bettoni, C. C., & de Oliveira, L. K. (2009). Nanoencapsulation increases quinine antimalarial efficacy against *Plasmodium berghei* in vivo. *International Immunopharmacology*, 9(8):1043–1049.
- Herr, J., Mehrfar, P., Schmiedel, S., & Wichmann, D. (2011). Reduced cardiac output in imported Plasmodium falciparum malaria. *Malaria Journal*, 10: 160.
- Herr, J., Mehrfar, P., Schmiedel, S., & Wichmann, D. (2011). Reduced cardiac output in imported Plasmodium falciparum malaria. *Malaria Journal*, 10(160):1–8.
- Holm, A. E., Wegener, A., & Gomes, L. C. (2022). Pulmonary and cardiac ultrasound findings among adults with uncomplicated malaria in the Amazon Basin. *The American Journal of Tropical Medicine and Hygiene*, 107(2):346–353.
- Iyawe, V. I., Ighodaro, O. M., & Akinrinlola, B. L. (2017). Short-term malaria infection and metabolic responses in Wistar rats. *African Journal of Biomedical Research*, 20(1), 45–51.
- Jimoh, A., Abdullahi, S., Dawoud, F., & Jimoh, A. O. (2022). Evaluation of the effect of resveratrol on parasitaemia in *Plasmodium berghei*-induced malaria in diabetic male Wistar rats. *Journal of Agripreneurship and Sustainable Development*, 5(3), 43–54.
- Joshi, R., Colford, J. M., & Reingold, A. L. (2017). Cardiac involvement in Plasmodium falciparum malaria. *Transactions of the Royal Society of Tropical Medicine and Hygiene*, 111(4):175–181.

- Katsoulis, O., Georgiadou, A., & Cunnington, A. J. (2021). Immunopathology of acute kidney injury in severe malaria. *Frontiers in Immunology*, 12:651739.
- Kaya, M., Çetinkaya, M. A., & Besne, D. (2024). The quantitative evaluation of cardiac structures and major thoracic vessel dimensions by means of lateral contrast radiography in Wistar albino rats (*Rattus norvegicus*). *DergiPark*.
- Khan, A. I., Kapoor, A., Chen, J., Martin, L., & Rogazzo, M. (2018). The antimalarial drug artesunate attenuates cardiac injury in a rodent model of myocardial infarction. *Shock*, 49(6):697–706.
- Koh, C. C., Neves, E. G. A., de Souza-Silva, T. G., & Carvalho, A. C. (2023). Cytokine networks as targets for preventing and controlling Chagas heart disease. *Pathogens*, 12(2):171.
- Kotepui, M., Kotepui, K. U., Milanez, G. D. J., & Masangkay, F. R. (2020). Cardiovascular and other complications associated with *Plasmodium vivax* malaria: A systematic review and meta-analysis. *BMC Infectious Diseases*, 20:363.
- Kwansah-Obresi, J. H., Moomin, A., Forkuo, A. D., & Sarpong, J. O. (2025). In vivo anti-plasmodial activity of alpha-onocerin and artesunate combination against *Plasmodium berghei*-infected mice. *Advances in Traditional Medicine*.
- Marrelli, M. T., & Brotto, M. (2016). The effect of malaria and anti-malarial drugs on skeletal and cardiac muscles. *Malaria Journal*, 15: 524.
- Maslachah, L., & Widiyatno, T. V. (2019). Sequestration and histopathological changes of the lung, kidney and brain of mice infected with *Plasmodium berghei* that exposed to repeated artemisinin. *Universitas Airlangga Repository*.
- Meibalan, E., & Marti, M. (2017). Biology of malaria transmission. *Cold Spring Harbor Perspectives in Medicine*, 7(3):25452.
- Milner, D. A. (2018). Malaria pathogenesis. *Cold Spring Harbor Perspectives in Medicine*, 8(1):5569.

- Mishra, S. K., Behera, P. K., & Satpathi, S. (2013). Cardiac involvement in malaria: An overlooked important complication. *Journal of Vector Borne Diseases*, 50(3):232–235.
- Nguee, S. Y. T., Júnior, J. W. B. D., & Epiphanio, S. (2022). Experimental models to study the pathogenesis of malaria-associated acute respiratory distress syndrome. *Frontiers in Cellular and Infection Microbiology*, 12:899581.
- Nieman, A. E., de Mast, Q., Roestenberg, M., Wiersma, J., & Wammes, L. J. (2009). Cardiac complication after experimental human malaria infection: A case report. *Malaria Journal*, 8: 277.
- Nwokocha, C. R., Owu, D. U., & Nwokocha, M. I. (2012). Experimental malaria: The in vitro and in vivo blood pressure paradox. *Cardiovascular Journal of Africa*, 23(3):98–104.
- Odeyemi, O. M., Ogundare, A. O., & Olatunji, B. P. (2021). Therapeutic efficacy of polyphenol-rich extract of *Gongronemalatifolium* in malaria-induced oxidative stress in rats. *African Journal of Traditional, Complementary and Alternative Medicines*, 18(3):89–97.
- Ogunro, P. S., Adebayo, K. A., & Sanya, A. E. (2023). Antioxidant enzyme status and lipid peroxidation in *Plasmodium falciparum* malaria-infected patients: A comparative study. *Nigerian Journal of Health Sciences*, 23(1):1–8.
- Ojha, V., Bansal, A., & Aggarwal, P. (2021). Malaria and the heart: A neglected area of research. *Tropical Medicine and Infectious Disease*, 6(3):139.
- Okafor, U. E., Ufele, A. N., & Nwankwo, O. D. (2019). Effects of artemisinin-based combination therapy on histopathology of the liver, kidney and spleen of mice infected with *Plasmodium berghei*. *Animal Research International*, 16(3):3480–3488.
- Olanlokun, J. O., Abiodun, W. O., & Ebenezer, O. (2022). Curcumin modulates multiple cell death, matrix metalloproteinase activation and cardiac protein release in susceptible and resistant *Plasmodium berghei* strains. *Infection, Genetics and Evolution*, 99:105250.

- Olatunji, G., Kokori, E., Ogieuhi, I. J., & Akinmoju, O. (2025). Myocarditis in malaria—current evidence and future directions: A literature review. *The Egyptian Journal of Internal Medicine*, 37(1):34.
- Olorunnisola, O. S., Afolayan, A. J., & Eloff, J. N. (2019). N-acetylcysteine ameliorates hepatic and renal oxidative damage in *Plasmodium berghei*-infected Wistar rats. *BMC Complementary and Alternative Medicine*, 19(1):57.
- Oluwatimilehin, O. E. (2024). Assessment of serum biomarkers of cardiac function (creatine kinase and troponin) in Wistar rats treated with Long Jack Sperm Enhancer.
- Opara, E. C., Emeji, R., & Egbujo, E. C. (2021). Oxidative stress and inflammation in malaria: Implications for treatment. *Journal of Biomedical Research and Clinical Practice*, 4(1):29–38.
- Otto, T. D., Böhme, U., Jackson, A. P., Hunt, M., Franke-Fayard, B., Hoeijmakers, W. A. M., ... Pain, A. (2018). A comprehensive evaluation of rodent malaria parasite genomes and their association with disease pathogenesis. *BMC Biology*, 16: 70.
- Otun, S. O., Graca, R., & Onisuru, O. (2024). Evaluation of *Plasmodium berghei* models in malaria research. *Signaling Journal*, 5(7).
- Oyeyemi, I. T., Sulaimon, L. A., & Olatunde, A. A. (2020). Anti-inflammatory and antioxidant potential of turmeric (*Curcuma longa*) extract in rodent model of malaria. *Phytomedicine Plus*, 1(1):100003.
- Parroche, P., Lauw, F. N., Goutagny, N., Latz, E., Monks, B. G., Visintin, A., ... Golenbock, D. T. (2007). Malaria hemozoin is immunologically inert but radically enhances innate responses by presenting malaria DNA to Toll-like receptor 9. *Proceedings of the National Academy of Sciences*, 104(6):1919–1924.
- Pasini, E. M., & Kocken, C. H. M. (2021). Parasite-host interaction and pathophysiology studies of the human relapsing malarias *Plasmodium vivax* and *Plasmodium ovale* infections in non-human primate models. *Frontiers in Cellular and Infection Microbiology*, 10: 614122.

- Pongponratn, E., Turner, G. D. H., Day, N. P. J., Phu, N. H., Simpson, J. A., Stepniewska, K., ... White, N. J. (2012). An ultrastructural study of the brain in fatal *Plasmodium falciparum* malaria. *American Journal of Tropical Medicine and Hygiene*, 86(5):718–726.
- Popa, G. L., & Popa, M. I. (2021). Recent advances in understanding the inflammatory response in malaria: A review of the dual role of cytokines. *Journal of Immunology Research*, 21(10):1–9.
- Popa, G. L., & Popa, M. I. (2021). Recent advances in understanding the inflammatory response in malaria: A review of the dual role of cytokines. *Journal of Immunology Research*, 11:180.
- Ray, H. N., Doshi, D., Rajan, A., & Singh, A. K. (2017). Cardiovascular involvement in severe malaria: A prospective study in Ranchi, Jharkhand. *Journal of Vector Borne Diseases*, 54(2):174–178.
- Rezende, L. M. T., Soares, L. L., & Drummond, F. R. (2021). Is the Wistar rat a more suitable normotensive control for SHR to test blood pressure and cardiac structure and function? *International Journal of Cardiovascular Sciences*, 34(1):16–24.
- Ribeiro, S., Pereira, A. R. S., Pinto, A. T., & Rocha, F. (2019). Echocardiographic assessment of cardiac anatomy and function in adult rats. *Journal of Visualized Experiments*.
- Saadeh, K., Kumar, N. N., & Fazmin, I. T. (2022). Anti-malarial drugs: Mechanisms underlying their proarrhythmic effects. *British Journal of Pharmacology*, 179(4):801–815.
- Sanyaolu, A. O., Fagbenro-Beyioku, A. F., Oyibo, W. A., & Badaru, O. S. (2019). Malaria and myocarditis: A review of human cases. *Cardiology in Review*, 27(1):45–50.
- Sarma, A., Sinha, M., & Mitra, S. (2020). Cardiac pathology in malaria: A clinical update. *Journal of Tropical Cardiology*, 16(2):113–119.
- Sato, S. (2021). *Plasmodium*—a brief introduction to the parasites causing human malaria and their basic biology. *Tropical Medicine and Health*, 49(1), 21.

- Silva, L. S., Peruchetti, D. B., Silva-Filho, J. L., Souza, M. C., Henriques, M. D. G., Pinheiro, A. A., ... Abreu, T. P. (2013). Cardiac changes in *Plasmodium chabaudi* malaria in mice: Evidence of microvascular dysfunction and myocarditis. *Malaria Journal*, 12: 394.
- Silva-Santana, G., Aguiar-Alves, F., Silva, L. E., & Barreto, M. L. (2019). Compared anatomy and histology between *Mus musculus* (Swiss mice) and *Rattus norvegicus* (Wistar rats). *Preprints*.
- Simwela, N. V., & Waters, A. P. (2022). Current status of experimental models for the study of malaria. *Parasitology*, 149(4):392–405.
- Sinha, M., & Sarma, A. (2020). Cardiac pathology in malaria: Clinical insights and research updates. *Journal of Tropical Cardiology*, 16(2):113–119.
- Soniran, O. T., Idowu, O. A., & Ajayi, O. L. (2012). Comparative study on the effects of chloroquine and artesunate on histopathological damages caused by *Plasmodium berghei* in four vital organs of infected mice. *Malaria Research and Treatment*, 20: 758.
- Souza, A. C. M., Mosqueira, V. C. F., & Silveira, A. P. A. (2018). Reduced cardiotoxicity and increased oral efficacy of artemether polymeric nanocapsules in *Plasmodium berghei*-infected mice. *Parasitology*, 145(14):1883–1891.
- Souza, M. C., Silva, J. D., Pádua, T. A., & Capelozzi, V. L. (2013). Early and late acute lung injury and their association with distal organ damage in murine malaria. *Current Opinion in Pharmacology*, 13(3):361–369.
- Spichler-Moffarah, A., Ong, E., O'Bryan, J., & Solter, D. (2023). Cardiac complications of human babesiosis: Insights applicable to malaria-endemic areas. *Clinical Infectious Diseases*, 76(3):1385–1393.
- Thirumalasetty, S. S. (2024). Cardiac biomarkers in acute coronary syndrome. *International Journal of Health and Clinical Biomedical Science*, 5(2).
- Tuteja, R. (2007). Malaria – an overview. *FEBS Journal*, 274(18):4688–4697.

- Ukibe, N. R., Osakue, N. O., & Ukibe, E. G. (2024). Linking malaria and hypertension: Unveiling the interconnected pathophysiological nexus. *IDOSR Journal of Scientific Research*, 9(1):12–19.
- Umar, I. A., Saidu, Y., Bilbis, L. S., & Anigo, K. M. (2020). Antimalarial and antioxidant activities of *Ximenia americana* in *Plasmodium berghei*-infected mice. *BMC Complementary Medicine and Therapies*, 20(1):1–9.
- Vuong, P. N., Richard, F., Snounou, G., & Coquelin, F. (1999). Development of irreversible lesions in the brain, heart and kidney following acute and chronic murine malaria infection. *Parasitology*, 118(5):417–423.
- Walker, C., Deb, S., & Ling, H. (2020). Assessing the elevation of cardiac biomarkers and the severity of COVID-19 infection: a meta-analysis. *Journal of Pharmacology and Pharmaceutical Sciences*, 9(3):142–149.
- Wegener, A., Holm, A. E., Gomes, L. C., & Matos, L. O. (2022). Lung and cardiovascular changes in adults with uncomplicated *P. falciparum* malaria. *The American Journal of Tropical Medicine and Hygiene*, 107(3):579–586.
- Wu, X., & Dayanand, K. K. (2023). Different TLR signaling pathways drive pathology in experimental cerebral malaria vs. malaria-driven liver and lung pathology. *Journal of Leukocyte Biology*, 113(5):471–484.
- Zambare, K. K., & Thalkari, A. B. (2019). A review on pathophysiology of malaria: An overview of etiology, life cycle of malarial parasite, clinical signs, diagnosis and complications. *Asian Journal of Research in Pharmaceutical Sciences*, 9(3):123–129.

APPENDIX I

The instrument used for this research is as follows:

1. Animal House: during the time of feeding.
 - a. Feeding flat plate
 - b. Feeding water bottles
 - c. Feed (pellets)
 - d. ISOL disinfectant
 - e. Digital thermometer
 - f. Plastic cage
 - g. Weighing balance
 - h. Indian ink and plate

2. For Sacrificing
 - a. Hand gloves
 - b. Sterile Lancet
 - c. Cotton wool
 - d. Chloroform
 - e. Plastic container sterile with a cover
 - f. Dissenting set
 - g. Sterile containers
 - h. Formalin

3. Histology Laboratory
 - a. Scrape blade
 - b. Spatula
 - c. Block holder

- d. Automatic tissue processor
- e. Molten basket
- f. Tissue basket
- g. L-shaped mould
- h. Rotary type microtome
- i. Water bath
- j. Hot plate
- k. Metal pencil
- l. Slides and cover slip
- m. Stain (Haematoxylin and eosin)
- n. Binocular microscope
- o. Dibutylphthalate polystyrene xylene (DPX),
- p. Xylene, alcohol and water

APPENDIX II

- I. The mould was filled with molten paraffin wax
- II. With a pair of warm blunt-nosed forceps, tissues were transferred from the paraffin bath to the mould
- III. Forceps were warmed and tissues oriented until lying in the desired plane.
- IV. Corresponding labels from the paraffin bath were removed and placed against the side of the mould adjacent to the tissues.
- V. Air was blown on the surface until a thin film of wax has solidified.
- VI. The mould was transferred to a container of cold water and submerged until wax hardens.

After embedding, the block is left to harden up while placed on the ice for some hours before sectioning.

The Hertz microtome (Cambridge model) was used for trimming and sectioning at varying microns and the block clamp adjusted so that sections at 3-5 microns were obtained in a ribbon-like manner, which was floated in a water bath to flatten by gentle heat.

The section or short ribbon was picked using a clean grease-free slide to ensure that the sections were thoroughly dried before staining by placing on a hot plate. After which, slides were stained according to Hematoxylin and Eosin method.

APPENDIX III

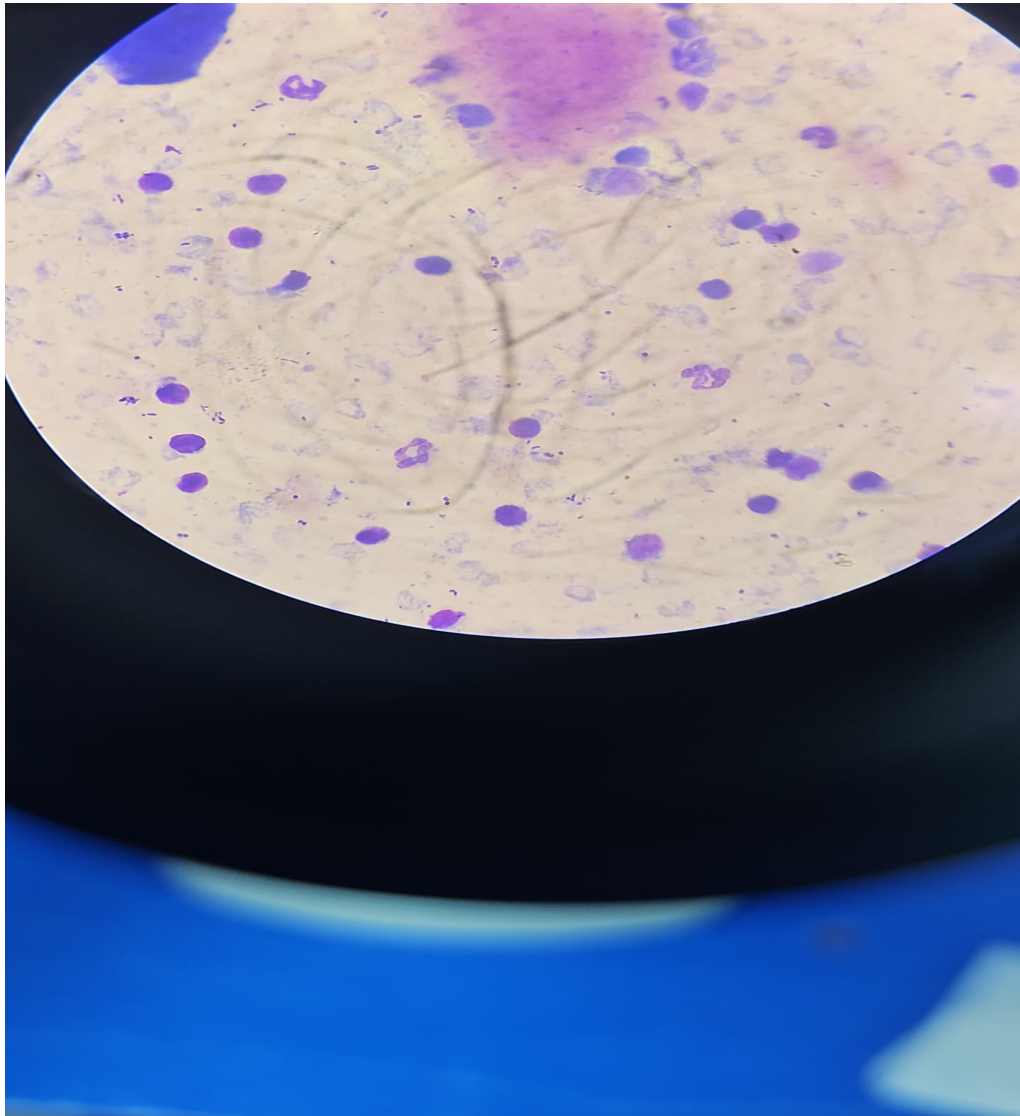
PROCEDURE FOR HEMATOXYLIN AND EOSIN STAINING

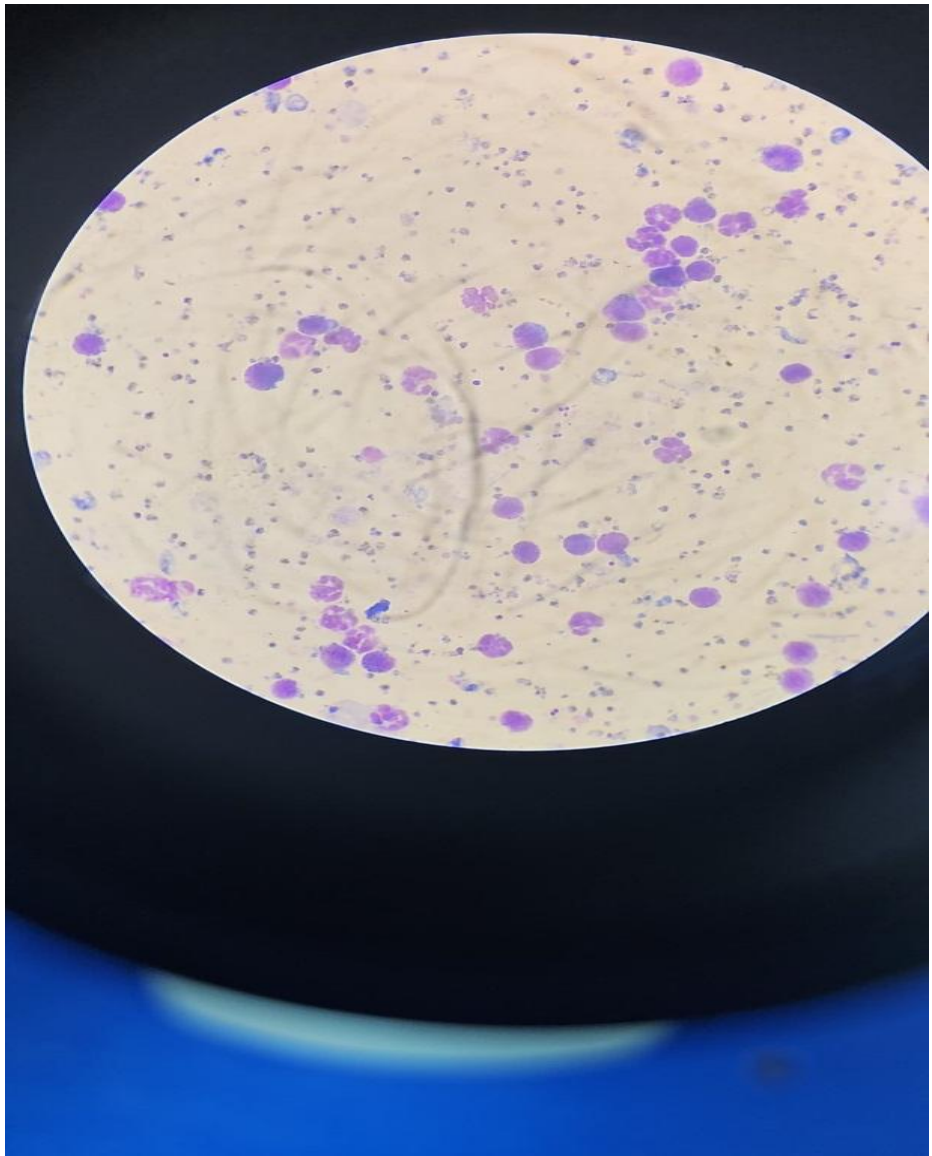
1. The section was dewaxed in two changes of xylene for 2minutes each.
2. The section were taken through descending grades of alcohol. From absolute alcohol for 2minutes to 90% alcohol for 1minutes, 70% alcohol for 1minutes
3. The slides were washed in running tap water for one minutes.
4. Tissue sections were stained in hematoxylin for 10minutes
5. The sections was rinsed in distilled water for 30 seconds.
6. The sections was then differentiated in 1% acid alcohol for 15seconds
7. After that, the sections were rinsed in distilled water for 5minutes.
8. The sections was counterstained with 1% eosin for 5minutes
9. The sections was washed in running tap water for 30seconds
10. Sections was dehydrated by passing through ascending grades of alcohol (70%, 90%, and 100%) for 1minutes each.
11. The section was cleared in two changes of xylene for 2minutes each
12. The section was mounted with DPX and viewed microscopically using the objectives lens.

APPENDIX IV

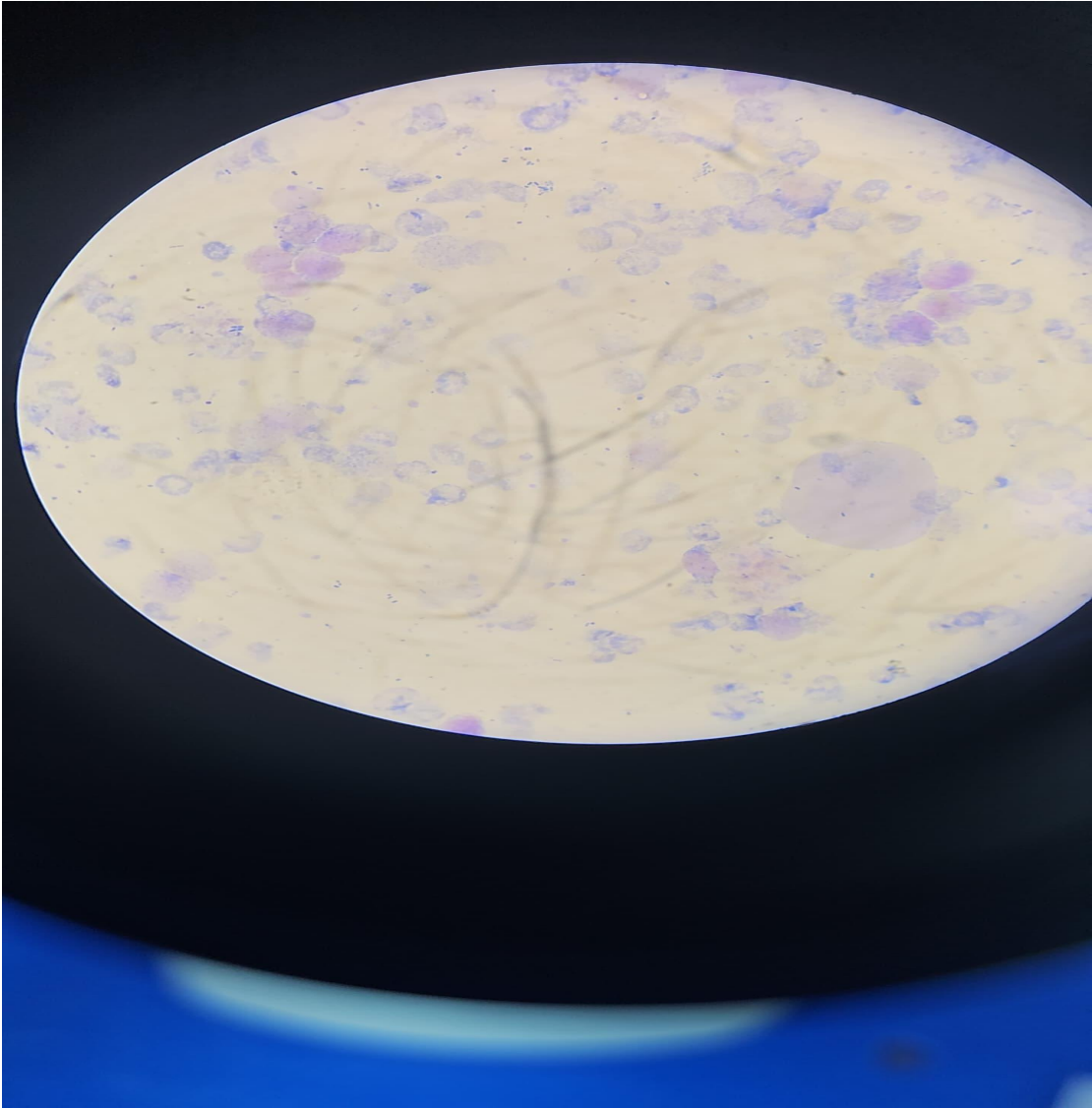
PARASITOLOGY RESULT OF MALARIA PARASITE

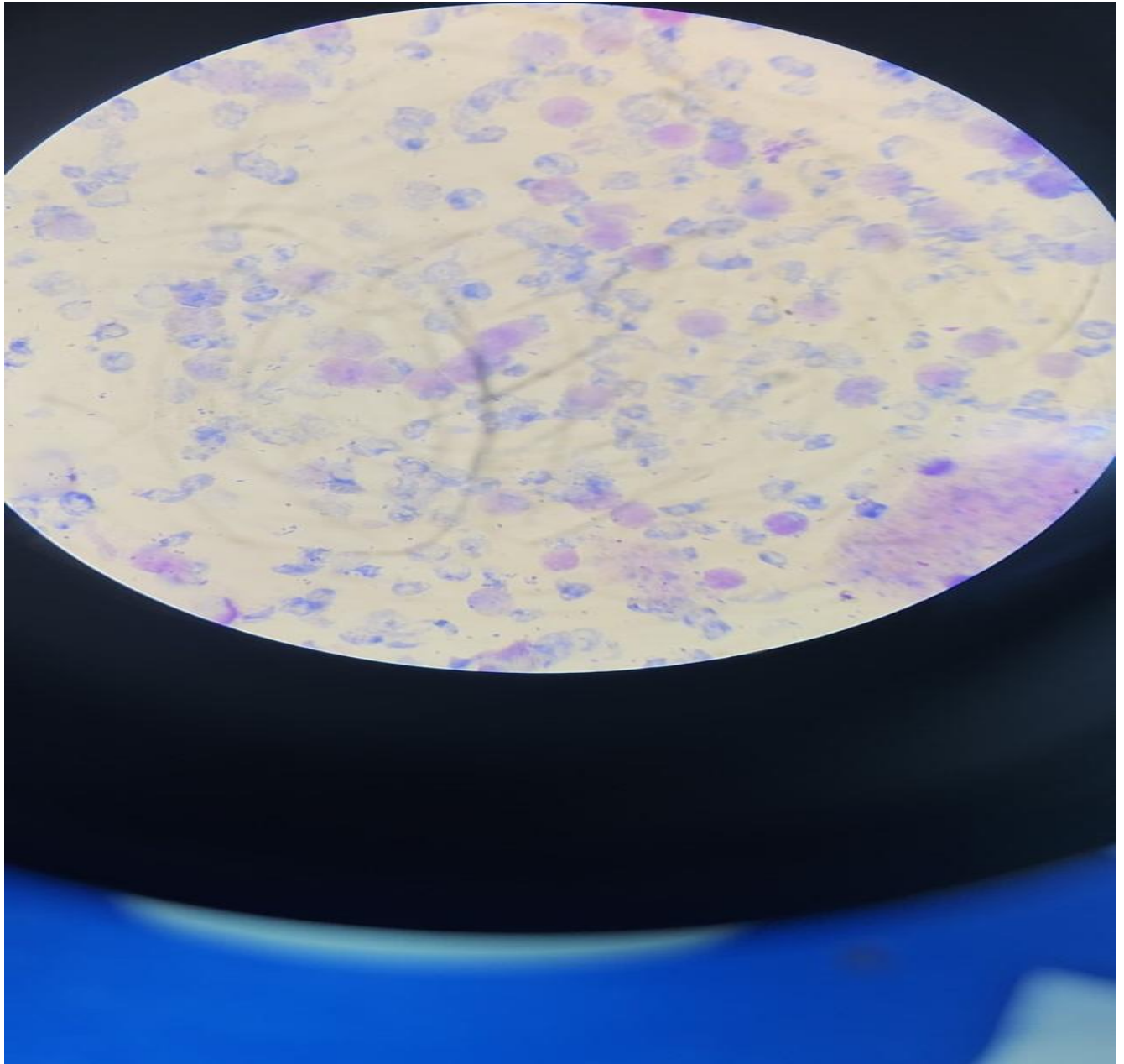
GROUP A



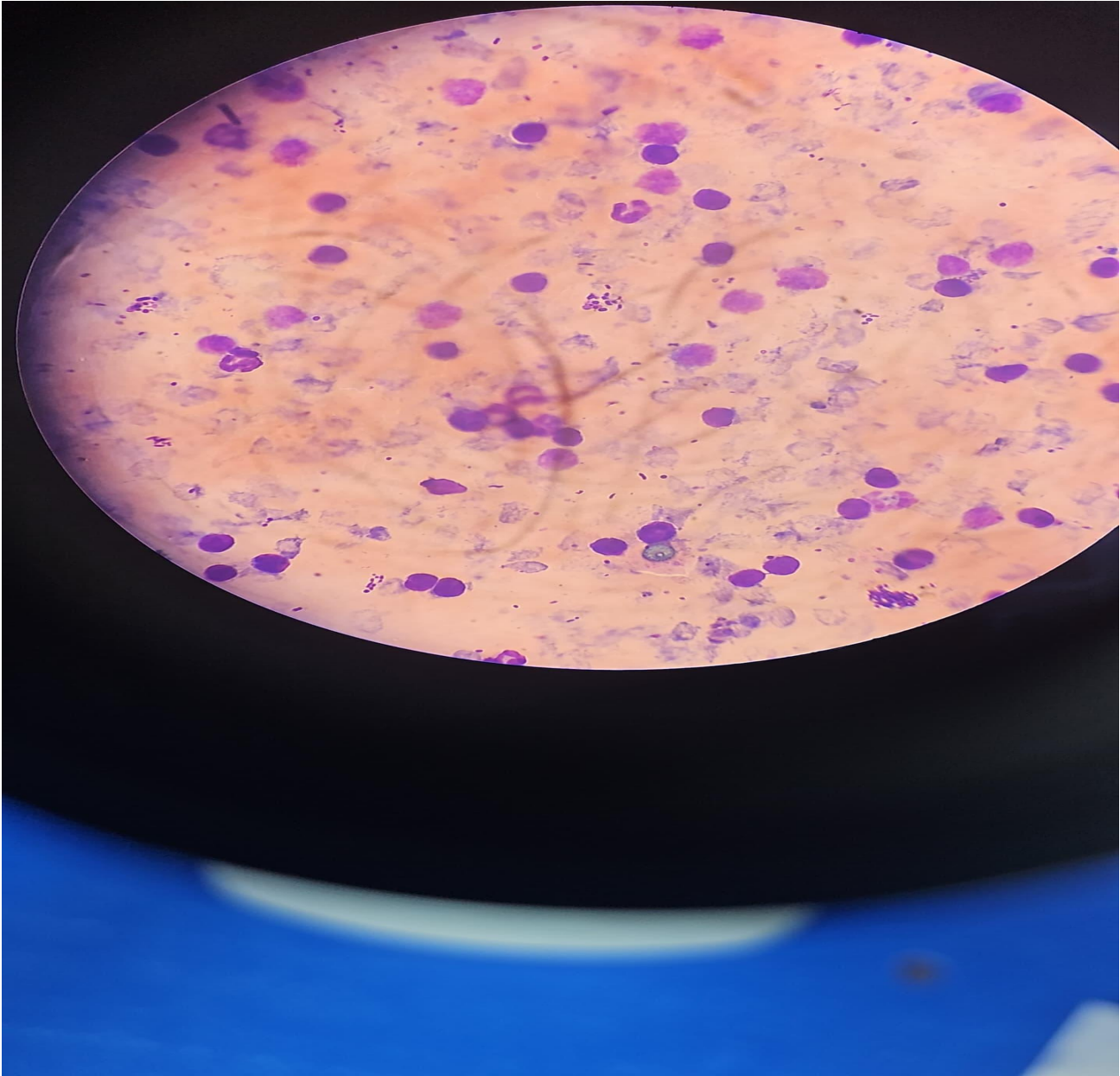


GROUP B

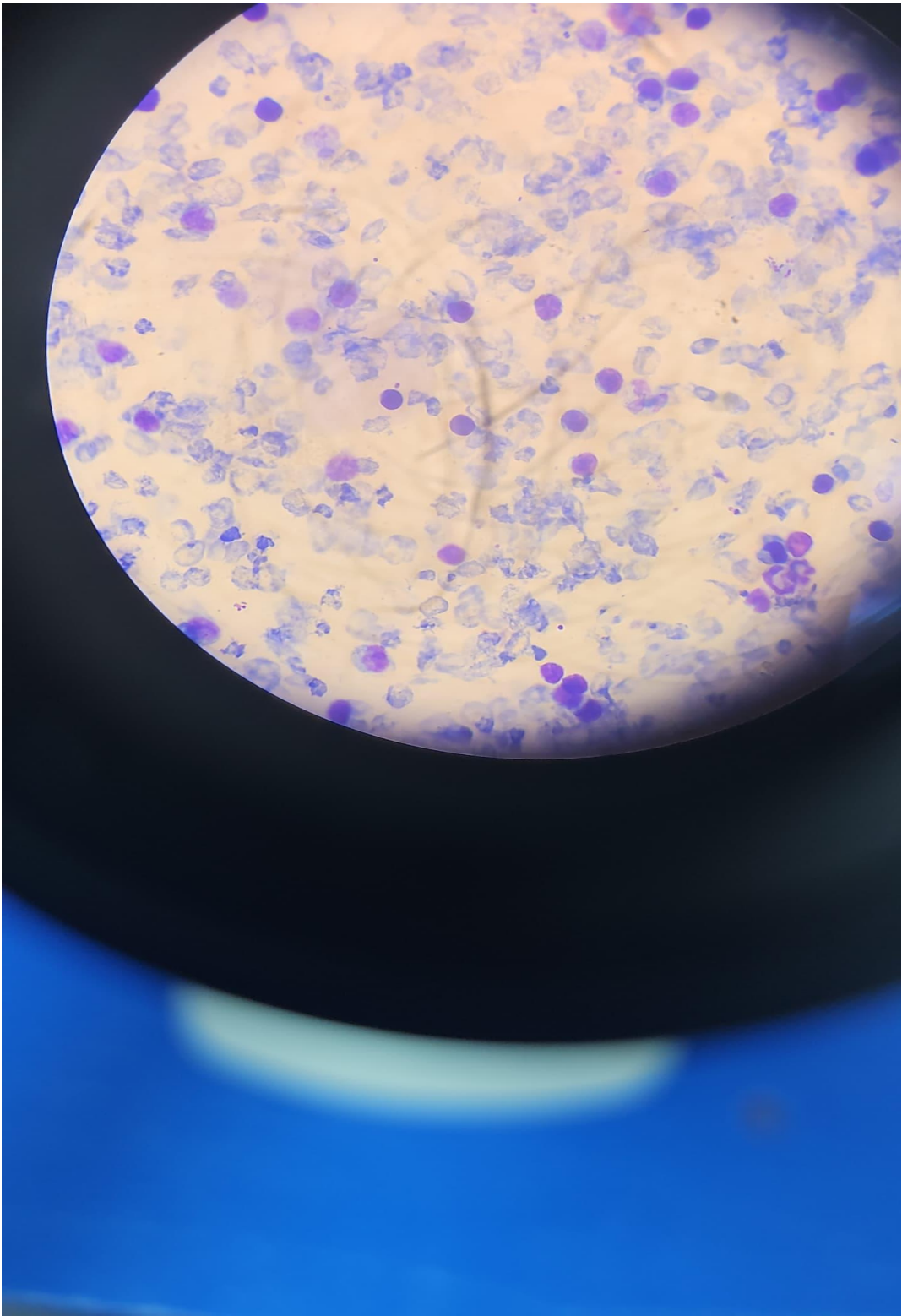




GROUP C



GROUP D



APPENDIX V

